ARTICLE IN PRESS

Progress in Biophysics and Molecular Biology xxx (xxxx) xxx

Contents lists available at ScienceDirect

Progress in Biophysics and Molecular Biology

journal homepage: www.elsevier.com/locate/pbiomolbio

An overview of the intracellular localization of high-Z nanoradiosensitizers

Mohammad Varzandeh [a], Sheyda Labbaf [a,*], Jaleh Varshosaz [b,**], Sophie Laurent [c]

[a] Department of Materials Engineering, Isfahan University of Technology, Isfahan, 84156-83111, Iran
[b] Novel Drug Delivery Systems Research Center and Department of Pharmaceutics, School of Pharmacy, Isfahan University of Medical Sciences, Isfahan, Iran
[c] Laboratory of NMR and Molecular Imaging, Department of General, Organic Chemistry and Biomedical, University of Mons, Mons, Belgium

ARTICLE INFO

Keywords:
Nanoradiosensitizer
Cell-nanomaterial interaction
Intracellular targeting
Radiation therapy

ABSTRACT

Radiation therapy (RT) is a method commonly used for cancer treatment worldwide. Commonly, RT utilizes two routes for combating cancers: 1) high-energy radiation to generate toxic reactive oxygen species (ROS) (through the dissociation of water molecules) for damaging the deoxyribonucleic acid (DNA) inside the nucleus 2) direct degradation of the DNA. However, cancer cells have mechanisms to survive under intense RT, which can considerably decrease its therapeutic efficacy. Excessive radiation energy damages healthy tissues, and hence, low doses are applied for cancer treatment. Additionally, different radiosensitizers were used to sensitize cancer cells towards RT through individual mechanisms. Following this route, nanoparticle-based radiosensitizers (herein called nanoradiosensitizers) have recently gained attention owing to their ability to produce massive electrons which leads to the production of a huge amount of ROS. The success of the nanoradiosensitizer effect is closely correlated to its interaction with cells and its localization within the cells. In other words, tumor treatment is affected from the chain of events which is started from cell-nanoparticle interaction followed by the nanoparticles direction and homing inside the cell. Therefore, passive or active targeting of the nanoradiosensitizers in the subcellular level and the cell-nano interaction would determine the efficacy of the radiation therapy. The importance of the nanoradiosensitizer's targeting is increased while the organelles beyond nucleus are recently recognized as the mediators of the cancer cell death or resistance under RT. In this review, the principals of cell-nanomaterial interactions and which dominate nanoradiosensitizer efficiency in cancer therapy, are thoroughly discussed.

1. Introduction

Cancer is the second leading cause of death worldwide and has a high rate of spread each year (Sung et al., 2021). Irregular proliferation, apoptosis inhibition mechanisms, angiogenesis, metastatic behaviour, growth independent of growth factors and non-responsiveness to cellular division suppressors are the principal hallmarks of cancer (Hanahan and Weinberg, 2000). A wide range of therapeutic methods have been developed to remove malignant tumors and prevent death. Surgery, radiation therapy and chemotherapy are the major therapeutic modalities to treat cancer owing to their effectiveness and availability (Abbas and Rehman, 2018). However, they are suffering from systemic or bystander organ damages (Li et al., 2021).

The introduction of novel treatment methods and the enhancement of common clinical therapies by means of nanotechnology concepts has recently gained attention (Rancoule et al., 2016). High electron density of the High-Z nanoradiosensitizers evokes a higher dose delivery followed by an intense chemical and biological effects. Parameters correlated to the radiosensitizer characteristics(e.g. atomic number, size), radiation parameters (e.g. energy of the beam) and subcellular localization of the nanoradiosensitizer were the three major factors modulating the dose enhancement factor (DEF) (Cai et al., 2013; Guidelli and Baffa, 2014; Hossain and Su, 2012). DEF is defined as deposited dose within tumors containing nanoradiosensitizer divided by the deposited dose in blank condition.

Thus, controlling the nanoradiosensitizer characteristics and the large X-ray attenuation coefficient of high-Z nanomaterials (titanium to bismuth with Z = 22 and 83, respectively) evokes efficient tumour

* Corresponding author. Department of Materials Engineering, Isfahan University of Technology, Isfahan, 84156-83111, Iran.
** Corresponding author. Department of Pharmaceutics, Faculty of Pharmacy and Novel Drug Delivery Systems Research Center, Isfahan University of Medical Sciences, Isfahan, PO Box 81745-359, Iran.
E-mail addresses: m.varzande@ma.iut.ac.ir (M. Varzandeh), s.labbaf@iut.ac.ir (S. Labbaf), varshosaz@pharm.mui.ac.ir (J. Varshosaz), sophie.laurent@umons.ac.be (S. Laurent).

https://doi.org/10.1016/j.pbiomolbio.2022.08.006
Received 27 December 2021; Received in revised form 17 July 2022; Accepted 19 August 2022
Available online 24 August 2022

ablation (Schuemann et al., 2020).

Nanoparticles interact with the cell membrane, which is an amphiphilic lipid barrier that protects the intracellular components, as the preliminary step to accomplish their predesigned mission (Contini et al., 2018). Additionally, the properties of the nanoparticles (e.g., size, shape and surface charge) are pivotal factors that simultaneously affect their interactions and cellular functions (Shao et al., 2017). The intracellular fate of nanoparticles greatly influences their therapeutic and regenerative functions (Labbaf et al., 2011; Ma et al., 2016; Tsigkou et al., 2014). As schematically illustrated in Fig. 1, the interactions between nanoradiosensitizers and cancer cells and their subcellular localization determines the cancer treatment efficacy.

2. Nanoradiosensitizers

High-Z element-incorporated nanoradiosensitizers fortify the cancer treatment by three main mechanisms: 1) Physical enhancement, 2) chemical enhancement and 3) biological enhancement. High-Z elements contains a huge number of electrons per atom (compare with water), endowing an increased attenuation cross-section. In the other words, physical enhancement of the high-Z elements refers to the absorbing more energy in comparison with water (in routine RT), which increases the generation of Compton, photoelectric and Auger electrons to the tumor (Chen et al., 2019a). The released electrons interact with water molecules and biomolecules, leading to the generation of cytotoxic reactive oxygen species (ROS) (Kempson, 2021). Regarding to the high reactivity of the as-produced ROS, it can elicit severe chemical modifications such as helical-structured DNA aberration and mitochondrial membrane oxidation. Also, biological enhancement indicates the effect of nanoradiosensitizers on the molecular and cellular pathways. Thus, the complex crosstalk between RT, cellular constitution and the biochemical/physical properties of the tumour determines the outcome of therapy. Radiosensitizers are organic or inorganic materials used to sensitize cancer cells to RT. Several subcellular effects of nanoradiosensitizers have been proposed and can be classified based on whether they induce DNA aberration, inhibit the DNA repair mechanism or interact with cellular compartments (Giocanti et al., 1993). As previously discussed, DNA damage is the most effective and well-known anticancer mechanism that benefits from the production of large amounts of electrons using Compton, photoelectric and Auger effects. Following this route, a wide range of nanoparticles (NPs) that interact closely with radiation has emerged (Wang et al., 2018). These NPs are mostly high-Z NPs, which are synthesized in various shapes and surface modifications.

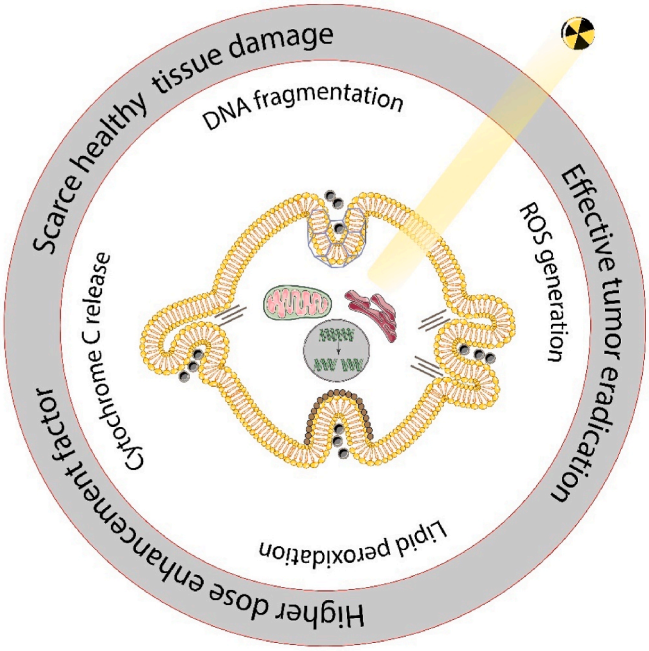

Fig. 1. Schematic representation of how cell-nanomaterial interactions and intracellular targeting affect the efficacy of nanoradiosensitizers.

3. Mechanisms of NP uptake

NPs interact with the cell outer membrane, and its multiple superficially exposed components, such as glycoproteins, can determine the intracellular fate of the particles. Generally, in a process called endocytosis, NPs are taken up by the cell and internalized in the cell organelles. There are several major endocytotic routes, such as phagocytosis, clathrin-mediated endocytosis, caveolin-mediated endocytosis, clathrin/caveolin-independent endocytosis and macropinocytosis (Fig. 2-A). Moreover, several laboratory techniques have been utilized to increase the permeability of the cell membrane and transfer NPs into the cytoplasm. Lipid fusion, electroporation and microinjection are among the commonly used procedures (Fig. 2-B). However, these methods suffer from cellular damage and complicated administration (Ho et al., 2021).

3.1. Clathrin-mediated endocytosis

Clathrin is a protein that resides on the cell membrane and is capable of self-polymerization. It consists of three heavy and three light chains that build a triskeleton, potentiating polymerization into sheet-like and cage-shaped structures. Clathrin-mediated endocytosis is the major way metabolites, hormones and proteins are received by cells. Clathrin-mediated endocytosis includes several steps: nucleation, invagination, scission and uncoating (Taylor et al., 2011). In the nucleation step, the interaction between the NPs and receptors stimulates nucleation on the cell surface through adaptor proteins to form a curved pit (Schmid et al., 2006). In the absence of clathrin and other cytosolic proteins, the formed pit is not sufficiently stabilized to proceed to the invagination step (Ehrlich et al., 2004). Next, dynamin, a specific membrane guanosine triphosphatase (GTPase), is recruited for scissoring the nanometer-sized vesicles (Praefcke and McMahon, 2004). GNPs bearing 20 nm(Ng et al., 2015) and 50 nm size (Chithrani and Chan, 2007) were shown to follow clathrin mediated endocytosis for cellular internalization.

3.2. Caveolae-mediated endocytosis

Caveolae are 50–100 nm invaginated lipid rafts within the cellular membrane. Caveolae formation is strictly dependent on the presence of the caveolins (the proteins caveolin-1, caveolin-2 and caveolin-3) expressed as a caveolae coating on the inner side of adipocytes and endothelial and fibroblast cells (Pelkmans and Zerial, 2005). Therefore, there is no need for protein recruitment, which is required for clathrin-mediated endocytosis. Caveolae-mediated endocytosis is the main mechanism involved in lipid regulation, cell signalling and vesicle transport. This mode of cell trafficking intervenes during the progression of several diseases, such as cancer and diabetes (Bae et al., 2019; Goetz et al., 2008; Savage et al., 2007). On the other hand, inhibiting caveolae causes pulmonary, muscle and lipid diseases (Le Lay and Kurzchalia, 2005). Notably, NPs trafficked via caveolae are prone to lysosomal degradation, which could be utilized for smart drug delivery systems (Karimi et al., 2016; Rejman et al., 2006). Cysteine modified-Gold (4.5 nm size)(Hao et al., 2012), silver (50 nm) (Bouallegui et al., 2018) NPs are the examples of the NPs endocytosed by this mode of endocytosis.

3.3. Clathrin-caveolae-independent endocytosis

This type of endocytosis occurs in cells that lack both clathrin and

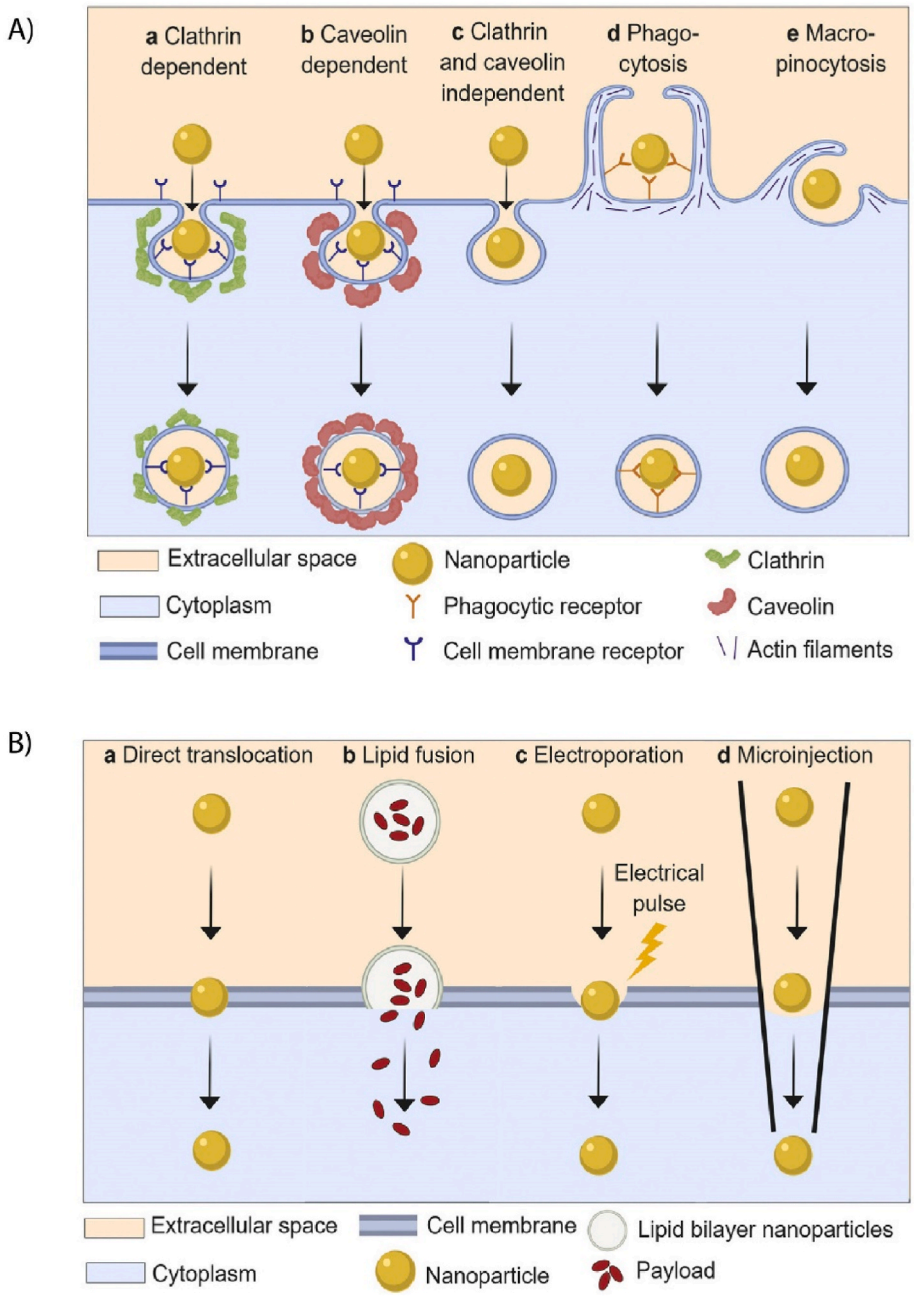

Fig. 2. A) Schematic illustrations of nanoparticle endocytosis into cells: (a) clathrin-dependent, (b) caveolin-dependent, (c) clathrin/caveolin-independent, (d) phagocytosis and (e) macropinocytosis. (Reproduced with permission from ref. (Donahue et al., 2019). Copyright Elsevier 2019.) B) Schematic representation of various methods for the cytoplasmic delivery of nanoparticles. (Reproduced with permission from ref. (Donahue et al., 2019). Copyright Elsevier.)

caveolae. These cells with a particular lipid composition take up biological agents such as interleukin-2, hormones and cellular fluids. This route is also responsible for introducing a variety of viruses such as severe acute respiratory syndrome (SARS) coronavirus (Wang et al., 2008) and simian virus (SV) 40 (Damm et al., 2005). Caveolae independent endocytosis was evidenced in PEGylated GNPs bearing 40–80 nm size (Li and Monteiro-Riviere, 2016).

3.4. Macropinocytosis

Micropinocytosis imports a large volume of extracellular fluids via engulfment. In this approach, the cytoskeleton rearranges into a specific shape, creating an enlarged vesicle (0.2–5 μm) following closure. Actin filaments obviate this reconfiguration procedure accompanied by receptor intervention, implying nonspecific uptake (Lee and Knecht, 2002). Therefore, NPs residing in extracellular fluids are engulfed without a ligand–receptor interaction. The large diameters of the vesicles involved in macropinocytosis compared to clathrin/caveolae strongly suggests that macropinocytosis enables the uptake of micrometre-sized particles (Kuhn et al., 2014). Gold nanorods (White et al., 2022)(length: 36 nm, diameter: 12 nm) utilizes macropinocytosis to enter breast cancer cells.

3.5. Phagocytosis

Phagocytosis is mainly involved in immune cell functioning for pathogen or dead cell removal. Additionally, NPs have a high probability of absorbing proteins on their surface, including opsonins such as

immunoglobulins, complement proteins and other proteins (Aderem and Underhill, 1999). NPs are phagocytosed into body fluids post-opsonization via a mechanism similar to that driven by bacterial (or any foreign agent) elimination (Gustafson et al., 2015). Therefore, these NPs are prone to removal from the bloodstream and redirection to the reticuloendothelial system (RES). To avoid protein absorption on the surface of NPs, surface modification via hydrophilic polymers is often applied (Jokerst et al., 2011; Suk et al., 2016).

4. Active targeting of cancer cells

The cell membrane is the initial hurdle facing radiosensitizers from a cellular point of view. Selecting a reliable way to introduce nanoradiosensitizers inside the cell enhances their translation into the clinic. Cells express an abundance of receptors on their surface, which directly facilitates the interactions with soluble biological factors. Mimicking the targeted and facile internalization of soluble factors into cells, researchers have functionalized NP surfaces with relevant biological agents to facilitate uptake mechanisms. These biological cues include proteins, polysaccharides, peptides, aptamers and small molecules (Yoo et al., 2019). Namely, folic acid has been decorated on the surface of radiosensitizers to target folate receptor-expressing cells (Khoshgard et al., 2014). In addition, antibody and peptide decoration confers high specificity towards exclusive receptors. For example, antibodies such as cetuximab targeting epidermal growth factor receptor (EGFR) (Kao et al., 2014; Reda et al., 2019), anti-EGFR targeting EGFR (Liu et al., 2015a), and RGD targeting $\alpha_v\beta_3$ (Wu et al., 2017; Xu et al., 2012; Zhang et al., 2019a) have been used.

The functionalization of nanoradiosensitizers with elements that are consumed by cells is the second targeting approach. Following this route, highly demanded energy sources, such as glucose or galactose, facilitate cell penetration of the nanoradiosensitizer into different types of cancer cells (Geng et al., 2011, 2014; Kaur et al., 2013; Wang et al., 2013a; Zhu et al., 2015). Moreover, the consumption of glutamine by mitochondria to produce vital metabolites for cancer cell growth is of particular interest (Cluntun et al., 2017). Glutamine has the potential to target 4T1 breast cancer cells *in vivo* compared with folic acid- and glucose-capped bovine serum albumin (BSA)/GNPs (Kefayat et al., 2019).

Choosing an appropriate targeting moiety depends on the cell and NP characteristics. Kong et al. (2008) visualized the interaction between cystamine- and glucose-modified nanoradiosensitizers and MCF-7 cells and the subsequent radiosensitization effect. Their results demonstrated that the glucose-capped NPs penetrated into the cytoplasm while the cystamine-modified NPs were adsorbed electrostatically onto the cell membrane.

5. Key factors modulating cell-nanoparticle interaction

5.1. Particle size

Particle size is the major characteristic governing the physical interaction between NPs and cells and their intracellular fate. Additionally, size-dependent cellular uptake affects the blood circulation half-life and body distribution of NPs. Phagocytosis favours the uptake of larger particles ($\approx 500\ nm$) by phagocytes, which are rapidly eliminated from the bloodstream (Hoshyar et al., 2016). NP size is crucial for passage through the blood–brain barrier (BBB) and gastrointestinal barrier, with an optimum size of $\approx 100\ nm$ (Kulkarni and Feng, 2013).

5.2. Shape

A deep understanding of nanoscience along with the vast development of laboratory instruments has made the synthesis of NPs of various shapes possible. The shape of a NP is a crucial factor modulating its interaction with the phospholipid bilayer, which could be leveraged for cancer cell-specific targeting (Cong et al., 2021). Namely, spherical GNPs with 74 nm and 14 nm in size were more favoured by HeLa cells than rod GNPs with dimensions of 74 × 14 nm (Chithrani et al., 2006). Qiu et al. (2010) showed that the cellular uptake velocity of rod-shaped GNPs by MCF-7 cells with dimensions of 14 × 51 nm, 17 × 50 nm, 21 × 40 nm and 30 × 33 nm was accelerated with a decrease in the aspect ratio. Therefore, it was postulated that rod-shaped nanoparticles require a longer uptake time when the aspect ratio increases owing to the time-consuming engulfment process (Chithrani and Chan, 2007). Xie et al. (2017) demonstrated that GNPs with a constant hydrodynamic size but different shapes (stars, rods and triangles) followed different endocytosis mechanisms into RAW264.7 cells. The uptake ratios of these differently shaped NPs followed the order from high to low of triangles, rods and stars. Additionally, recent studies have proven that the shape (spherical *vs.* star-shaped GNPs 50 nm in size conjugated with the AS1411 DNA aptamer) of NPs modulates their translocation in cells. Among GNPs with the same protein corona profile, those that were star-shaped were endocytosed faster by nucleolin-expressing cells (Choo et al., 2021).

5.3. Surface functional groups

As previously mentioned, the interaction between NPs and cells is highly dependent on the surface functionalities (Vergallo et al., 2016). In a study by Hu et al. (2018), Ag and Au, with the same size and charge, exerted different cell surface protein interactions. Therefore, beyond their size and charge, the nature of metallic nanoparticles is important. Glucose-coated Ag-NPs showed more toxicity than glucose-sucrose-coated Ag-NPs towards HeLa cells (Dini et al., 2011). Surprisingly, at lower concentrations (2×10^3 NPs/cell), the NPs induced autophagy, while an increase in the concentration (2×10^4 NPs/cell) caused the cellular death mechanism to change to necrosis (Panzarini et al., 2015). Autophagy-dominated cell death was evidenced in citrate-capped Ag-NPs *in vivo* (Mao et al., 2018). Additionally, cell cycle arrest has been proven to occur in glucose-capped Ag-NPs (Panzarini et al., 2017). Ultrasmall NP uptake is energy-dependent, and surface functionalization is a pivotal factor influencing protein corona adsorption and cell interactions (Muraca et al., 2020). Of note, the adsorption of several proteins (e.g., immunoglobins, opsonins, complement proteins) may be dependent on the surface functional groups, modulating nanoparticle elimination through the immune system (Mahmoudi et al., 2011b). Furthermore, the protein corona is one of the main factors affecting the toxicity of nanoparticles (Mahmoudi et al., 2012).

6. The role of cell-nanomaterial interactions in NP radiosensitization

6.1. Gold NPs (GNPs)

GNPs have been widely used for various biomedical applications owing to their relatively high biocompatibility, facile surface modification and surface plasmon resonance effects (Karimi et al., 2019). Additionally, their shape- and size-dependent physical properties have been leveraged for versatile applications (e.g., biosensors) (Zhang et al., 2012b). Due to the proteins adhered to the surface of the NPs, the uptake of GNPs is usually dominated by receptor-mediated endocytosis (Alhussan et al., 2021).

Zhang et al. (2012a) reported higher HeLa cell internalization of 12.1 and 27.3 nm PEG-coated GNPs than in 4.8 and 46.6 nm GNPs. Additionally, the 50 nm GNPs exerted more intensive cell death under radiation in comparison with 14 and 74 nm GNPs, owing to their higher uptake by HeLa cells (Chithrani et al., 2010). In contrast, some exceptions were reported in which NPs that were more easily internalized showed a lower death rate. Namely, introducing a similar dosage of 1.9 nm GNPs to DU145 and MDA-MB-231 cells led to higher internalization

by DU-145 cells. However, more cell death after radiation treatment was evidenced in MDA-MB-231 cells compared with no meaningful impact from radiation on DU-145 cells (Coulter et al., 2012). In addition, no induction of double strand breaks or interruption of repair was evidenced even at higher doses of incident radiation in this group (Jain et al., 2011). It is worth mentioning that a DNA/GNP mixture expressed DNA aberrations in size- and concentration-dependent manner, which demonstrates the importance of these factors (Brun et al., 2009). Additionally, the concentration of NPs introduced into the cell medium determines the amount of NP uptake (Liu et al., 2015b).

Generally, cell-specific nanoparticle uptake should not be neglected when using the radiosensitizing approach (Ahmad et al., 2020; Butterworth et al., 2010). Beyond their size, the shape of the NPs determines their interaction and internalization into cells. For instance, spherical NPs are more favoured by cells than those that are rod-shaped because spherical NPs can be endocytosed (Chithrani and Chan, 2007; Chithrani et al., 2006). Regarding the abovementioned early studies, PEG-coated GNPs, gold nanorods (GNRs) and gold nanospikes (GNSs) with minimal size variation showed versatile cellular trafficking in the order GNPs > GNSs > GNRs, which led to the respective descent in cellular death under radiation therapy (Ma et al., 2017b). GNR functionalization with antibodies rescues their scarce uptake and directs them to increase their tumour repositioning and radiosensitizing effects (Zhang et al., 2019a).

Evaluating cell radiosensitization under hypoxic conditions that mimic the natural tumour microenvironment would increase our knowledge base. Cui et al. (2014) evaluated GNP-treated cells treated with radiation under normoxic, acute hypoxic (4 h of incubation with 0.2% O_2) and chronic hypoxic (72 h of incubation with 0.2% O_2) conditions. Remarkable alterations in the numbers of dead cells under normoxic conditions versus hypoxic conditions (chronic and acute) may be attributed to the significant uptake of NPs. However, although the number of internalized NPs in both hypoxia groups was the same, a greater amount of cell death was evidenced in the chronic hypoxia group, which unveils the role of homologous recombination pathway impairment under chronic hypoxia (Cui et al., 2014). Studying the impact of various oxygen concentrations rather than the hypoxic duration would alter the population of internalized NPs. Thus, Jain et al. (2014) divided cells into three groups: normoxia, hypoxia and anoxia with 21%, 1% and 0.1% oxygen, respectively. Cell death was closely related to cellular uptake and followed the order normoxia, hypoxia and anoxia (Jain et al., 2014).

As mentioned before, the cell population in G2/M phase has increased cellular trafficking. Recently, Rieck et al. (2019) demonstrated the effects of cell phase distribution on cellular uptake. They found that cells synchronized in G1/S phase treated with 17 and 46 nm GNPs showed increased internalization and cell death under radiation treatment. Surprisingly, tricking the cells by designing Trojan nanolipids 50 nm in size (which are more favoured for uptake) carrying 5 nm GNPs accompanied by cell phase synchronization led to high cellular accumulation of the small GNPs (Bromma et al., 2019). The interaction of GNPs radiosensitizers with cells and their effect on cellular events is listed in Table (1).

6.2. Hafnium oxide NPs

Hafnium oxide NPs represent the most successful translation of NPs to clinical use. Nanobiotix developed hafnium oxide NPs (NBTXR3) as radiosensitization agents, passing the final levels of clinical trials (Anselmo and Mitragotri, 2016). Many *in vitro* and *in vivo* studies by this company remarked on the interaction of these NPs with biological media under radiation therapy. In detail, NBTRX3 is engineered to have a size of 50 nm and a spherical shape to increase cellular uptake through the previously discussed principles (Maggiorella et al., 2012). The NPs form clusters inside the endosome upon internalization (Maggiorella et al., 2012) as a function of concentration and cell line (Marill et al., 2014). As depicted in Fig. 3-A, the 42 MG-PA glioblastoma cell line has a higher number of clusters per cell than mesenchymal HT-29 cells (Marill et al., 2014). Moreover, the cluster size in PANC-1 cells (Fig. 3-B) was lower than that in 42-MG-BA cells (Fig. 3-C). Recently, Marill et al. (2019) reported that hafnium oxide-treated cells under radiation treatment undergo micronuclei formation following DSB induction. Micronuclei formation was confirmed to be associated with the cGAS-STING pathway. Additionally, spindle-like HfO_2 presented BAX upregulation both *in vivo* and *in vitro* in a study by Li et al. (2020). Surprisingly, these NPs were able to decrease cell proliferation, as represented by Ki-67 immunohistochemical staining.

Table 1
Cell-nanomaterial interactions of GNP radiosensitizers.

NP	Size	Conc.	Functionalization	Cell line(s)	Radiation	NP effects on cell(s)	Radiosensitization outcome	Reference
Gold	1.9	12 μM	-	MDA-MB-231, DU145 and L132 (immortalized)	3 Gy, 160 kVp	- Endocytotic uptake - Large endosomal aggregates observed - Cell death under radiation: DU145 > MDA-MB-231> L132	- No meaningful radiosensitization in DU145 or L132 cells	Coulter et al. (2012)
Gold	1.9	12 μM	-	MDA-MB-231, DU145 and L132 (immortalized)	6 MV (3.55 Gy/min), 15 MV (3.85 Gy/min), 6 MeV (4.0 Gy/min), and 16 MeV (4.0 Gy/min)	- No G2/M arrest - No meaningful DSB induction - Accumulation in the cytoplasm	- Sensitization in only MDA-MB-231 cells	Jain et al. (2011)
Gold	4.8, 12.1, 27.3 and 46.6 nm	0.05 mM, 0.1 mM	PEG	HeLa	662 KeV, 5 Gy (gamma ray)	- Higher uptake of the 12.1 and 27.3 nm NPs - PEG diminished the interaction with the cell membrane	- Higher SER for the 12.1 and 27.3 nm GNPs	Zhang et al. (2012a)
GNPs, GNSs and GNRs	GNPs (107.8 ±32.4), GNSs (118.1 ±46.4) and GNRs (108.9 ±50.6)	50 μg/ml	PEG	KB	6 MV, 200 cGy/min, 4 Gy	-Order of uptake: GNPs > GNSs > GNRs -Slightly increased G2/M phase arrest after radiation	- Order of cell death: GNPs > GNSs > GNRs	Ma et al. (2017b)

Table 2
Cell-nanomaterial interactions of gadolinium-based radiosensitizers.

Nanoparticle	Size (nm)	Conc.	Coating	Cell line(s)	Mechanism	Radiation	Note(s)	Ref.
Polysiloxane core with gadolinium chelates	3 ±1	0.5–2 mM	-	U87	Clathrin-mediated endocytosis	Gamma, 1.25 MeV	- Localized inside the lysosome - No accumulation in the nucleus or mitochondria	(Štefančíková et al., 2014)
Gadolinium hexanedione	140	100 μg/ml	-	Human mesenchymal stem cells	Endocytosis	N.A.	- The stem cell surface marker was protected	Tseng et al. (2010)
Polysiloxane core with gadolinium chelates	3	1 mM	-	U87	Endocytosis	1 Gy/min, 1–4 Gy	- Localized inside the cytoplasm - No difference in cytoplasm accumulation from 1 to 16 h	(Štefančíková et al., 2016)
Gadolinium-loaded chitosan	430	40 ppm (Gd conc.)	-	L929, B16F10, SCC-VII	Endocytosis	N.A.	- Endocytosis diminished at 4 °C	Shikata et al. (2002)
Polysiloxane core with gadolinium chelates	2.9 ± 0.2	0.1–2 mM	-	SQ20B	-	250 kV, 2 Gy/min	-Accumulated in the cytoplasm - Mitotic catastrophic cell death and decreased proliferation	Miladi et al. (2015)
Polysiloxane core with gadolinium chelates	3	0.5 mM	-	PANC-1	Endocytosis	220 kVp, 6 MV FFF, and 6 MV STD	- Observed in vacuoles in the cytoplasm	Detappe et al. (2015)

6.3. Gadolinium NPs

Gadolinium-based structures have been widely approved by the FDA as MRI contrast agents due to their paramagnetic characteristics (Bridot et al., 2007; Maravilla et al., 2017). Xcytrin, a gadolinium compound, has been used as a chemotherapeutic and radiosensitizing drug and is progressing through clinical trials (Korman et al., 2019). Recently, gadolinium-based NPs (GdNPs) were tested as theranostic agents owing to their high atomic number (Detappe et al., 2016). The exclusive properties of GdNPs led to the development of AGuIX with a polysiloxane core coated with Gd chelates as a theranostic agent by the company NH TherAguix (Lux et al., 2019). AGuIX acts as an MRI, X-ray computed tomography (CT) and single-photon emission CT (SPECT) contrast agent as well as nanoradiosensitizer nanoparticle (Dufort et al., 2015, 2016; Lux et al., 2011; Verry et al., 2016, 2019). Furthermore, many GdNPs have exhibited low reticuloendothelial removal, leading to extensive tumour accumulation and negligible renal toxicity (Kryza et al., 2011; Miladi et al., 2013; Sancey et al., 2015). The rapid translation of gadolinium-based theranostic agents necessitates the vital role of toxicity evaluations (Choi and Moon, 2019; Gheran et al., 2017; Ramalho et al., 2016).

Most cell-nanomaterial interactions with Gd-based NPs have focused on AGuIX analogues. Therefore, the interaction of AGuIX with cellular compartments is distinct from the pure or oxidized form of Gd. For instance, Mowat et al. (2011) observed that most DNA damage corresponded to treatment with 0.5 mM AGuIX with a moderate intracellular GdNP content compared with higher concentrations of AGuIX. Seeking to determine the mechanism leading to this effect, Rima et al. (2013) reported that two pathways dominate the cellular internalization of GdNPs: macropinocytosis and passive internalization. GdNPs agglomerate within vacuoles (with clarified membranes) or inside the cytoplasm with any membrane, as represented in Fig. 4-A, B, C. In this study, macropinocytosis showed a remarkable radiosensitization effect on cells, whereas passive diffusion was not sufficient to induce radiosensitization. The lamellipodia or arms of the macropinosome are well defined in Fig. 4-D. Notably, a high concentration of GdNPs diminishes cellular uptake and electron generation efficacy due to aggregate formation (Delorme et al., 2017; Mowat et al., 2011). In other words, the NP charge and concentration determine the interaction with the cell membrane as well as its aggregate formation. Other studies have determined that endocytosis is the dominant cellular uptake pathway, as indicated in Table (2).

Gd oxide NPs (GdONPs) of various shapes have gained broad attention in cancer therapy and diagnostics (Luo et al., 2020; Wu et al., 2019; Zhao et al., 2019). They are chemically and physically more stable than Gd-chelated NPs (Alizadeh et al., 2019). Additionally, their therapeutic efficiency is enhanced in combinational therapies. Namely, Zhao et al. (2019) synthesized Mn-doped GdO to extend the therapeutic window of both chemodynamic therapy and photothermal therapy (PTT) while maintaining MRI contrast ability. The Mn within the GdONP structure generates ROS via a Fenton-like reaction, increasing cell death in combination with PTT. Furthermore, modifying the imaging ability of the GdONPs was executed by doping with Er3+, Yb3+, Zn2+ and Tb3+ ions, which endows the NPs with an upconversion modality (Hemmer et al., 2013; Kamińska et al., 2015; Louis et al., 2005). In a study by Detappe et al. (2017), GdONPs/silica as a core/shell system was decorated with a Bi^{3+} chelate to simultaneously strengthen the CT imaging and radiosensitization properties.

In contrast to their high performance in cancer therapy and imaging, cell-nanomaterial interaction studies are limited. In a study by Miladi et al., 2.9 nm GdONPs increased the population of SQ20B cells in G2/M phase just after radiation administration. However, the phase distribution transformed to mostly sub-G1 phase in a dose-dependent manner at 240 h after radiation treatment (Miladi et al., 2015). In another study, 3 nm GdONPs arrested F98 cells in G2/M phase under irradiation (Taupin et al., 2015). These GdONPs exhibited cytotoxic autophagy-mediated radiosensitization in NH1299 cells (Li et al., 2019). With a similar size, NPs with a polysiloxane core conjugated with Gd chelates showed mitotic catastrophic cell death in SQ20B cells (Miladi et al., 2015). Recently, Shen et al. decorated GdO/polyacrylic acid/reductive bovine serum albumin with RGD dimers and lactoferrin to overcome the blood brain barrier (BBB). Initially, the LF receptor facilitated transcytotic action through the BBB, while RGD targeted brain tumors via the αvβ3 receptor. The endocytosed NPs ruptured the late endosome and accumulated in the area surrounding the nucleus. Moreover, X-ray irradiation triggered tumour volume reduction as detected by MRI (Shen et al., 2020).

7. Cell cycle effects

The cell cycle is a repeating cycle of stages that correspond to cell replication and division (Arata and Takagi, 2019). Beyond the DNA damage response, cells experiencing oxidative stress undergo cell cycle arrest (Kuczler et al., 2021). Different NPs interfere with the regulation

Table 3
Clinical trials of the radiosensitizers.

Nanoradiosensitizer	Targetted tumor	Trial ID	Phase	Number of patients	Root of injection	Dose of nanoradiosensitizer	Total dose of radiation	Year
NBTXR3	Liver cancer	NCT02721056	I–II	23	Intralesional (IL), intraarterial (IA)	IA: 10%, 15%, 22%, 33% and 45% (of the tumor volume) IL: 10%, 15%, 22%, 33% and 42% (of the tumor volume)	Stereotactic Body Radiation Therapy, 45 Gy (15 Gy x 3 fractions) or 50 Gy (10 Gy x 5 fractions)	2016–2020
	Prostate cancer	NCT02805894	I–II	5	Intraprostate	N/A	- Intensity modulated radiotherapy(IMRT): 45 Gy (1.8 Gy x 25) and fractions) with 34.2 Gy (1.8 Gy x 19 fractions) - Brachytherapy: (15 Gy x 1 fraction) + IMRT: 45 Gy (1.8 Gy x 25 fractions)	2017–2020
	Soft tissue sarcoma	NCT01433068	I	22	Intratumoral	N/A	50 Gy (2 Gy x 25 fractions)	2011–2020
	Metastatic NSCLC, Metastasis From Malignant Tumor of Bladder (Disorder), Metastatic Renal Cell Carcinoma etc.	NCT03589339	I	60	Intratumoral (combined with Anti-PD-1 drug)	N/A	Stereotactic Ablative Radiotherapy	2019–2023 (Recruiting)
	Adult Soft Tissue Sarcoma	NCT02379845	II–III	180	Intratumoral	N/A	5 weeks/50 Gy (5 × 2 Gy by week)	2015–2020
	Head and neck cancer	NCT01946867	I	63	Intratumoral	N/A	IMRT: 70 Gy (2 Gy x 35 fractions)	2014–2022 (Recruiting)
	Head and neck squamous cell carcinoma	NCT02901483	I–II	42	Intratumoral	5%, 10%, 15%, 22% and 33% (of the tumor volume)	70–72 Gy (2–2.12 Gy/ fraction)	2016–2022
PEP503	Rectal cancer	NCT02465593	I–II	42	Intratumor (Combined with 5-fluoro-uracil capecitabine)	N/A	IMRT and intensity modulated arc therapy (IMAT): 5000 cGy (200 cGy x 25) to gross tumor and nodes + 4500 cGy (180 cGy x 25) to pelvis	2015–2022
AGuiX	Multiple Brain Metastases	NCT03818386	II	100	Intravenous	100 mg/kg	30 Gy (3 Gy x 10 fractions)	2019–2022
	Brain metastases	NCT04899908	II	112	Intravenous	N/A	Stereotactic Radiation	2021 (Recruiting)
	Brain Metastases	NCT02820454	I	15	Intravenous	15, 30, 50, 75 and 100 mg/kg	30 Gy (3 Gy x 10 fractions)	2016–2019
	Gynecologic Cancer	NCT03308604	I	18	Intravenous	20, 30 and 50 mg/kg	External beam radiotherapy (EBRT): 45–57.5 Gy (In 5 wees) + Uterovaginal brachytherapy (15 Gy)	2017–2021
	Non-small Cell Lung Cancer, Advanced Pancreatic Adenocarcinoma, Unresectable Pancreatic Cancer and Ductal Adenocarcinoma of the Pancreas	NCT04789486	I-II	100	N/A	N/A	magnetic resonance imaging (MR)-guided stereotactic body radiation therapy (SBRT)	2021 (Recruiting)

of the cell cycle in individual ways (Mahmoudi et al., 2011a). Moreover, NP uptake is increased when the cells are in G2/M stage (Kim et al., 2012). Additionally, G2/M phase is the most radiosensitive phase; thus, arresting the cell cycle in this phase is essential (Pawlik and Keyomarsi, 2004). Notably, the cell cycle is altered following ionizing radiation induction, and hence, NPs that interfere with the cell cycle should be studied prior to and after radiation induction.

NPs present in cells in G2/M phase prior to radiation treatment have shown tremendous effects on radiosensitization-mediated death (Geng et al., 2011; Li et al., 2015a; Zhang et al., 2019b). However, less radiosensitization has been achieved by cells in G0/G1 phase, as represented by small GNP (1.9 nm)-treated cells (Butterworth et al., 2010; Coulter et al., 2012; Jain et al., 2011) and citrate-capped GNPs 14.8 nm in size (Liu et al., 2015b). Referring to the cell-nanomaterial interaction principals would assist in predicting NP behaviour towards cells.

Wang et al. (2013a) evaluated the S, G0/G1 and G2/M phases of A549 cells treated with glucose-GNPs, X-rays and both. Compared to the trend of cells residing in G2/M phase, a higher level of G2/M arrest was observed in glucose-GNP-treated cells in the radiation group. Similar results were previously reported by Roa et al. (2009), who reported that glucose-GNPs are responsible for G2/M arrest. Inhibition of P53 following radiation represents DNA aberration (Roa et al., 2009). Otherwise, P53 expression after radiation controls G2/M arrest (Lee et al., 2013). Owing to this concept, G2/M phase augmentation was determined after treatment with selenium NPs by Chen et al. (2018). The ratio of living cells in G2/M phase increased in a dose-dependent

Table 4
In-vivo studies of the intracellular targeted radiosensitizers.

Targetted organelle	Targeting moiety	Nanoparticle	Size (nm)	Cell line (Radiation dose)	Indication	In-vivo	Therapeutic outline	Ref.
Nucleus	TAT	Upconversion nanoparticle(NaYF4: Yb/Er/Tm/Gd)	< 50	MCF-7/ multidrug resistant MCF-7	ROS↑	MCF-7 tumor bearing nude mice	Relative tumor volume was decreased in targeted nanoparticle containing Mitomycin C to 0.5 (versus 2 in control)	Fan et al. (2015b)
	TAT	Upconversion nanoparticle(Y, Yb, Er, Tm and Gd elements)	< 40	HT-1080(5 Gy)	ROS↑ DNA damage (Comet assay)↑	HT-1080 bearing balb/c nude mice (6Gy)	Relative tumor volume was decreased in targeted nanoparticle radio-/ photo- senisitization to −50% (versus +600 % in control)	Fan et al. (2015a)
	αvβ3/TAT	Iridium nanocrystal	4	4T1(4–6Gy)	ROS↑ Fluorecence intensity↑	female Kunming mice(8Gy)	- Tumor was completely removed in synergized photothermal and radiosensitization (versus ∼ +255 % in control) - No adverse histopathologic damage	Wang et al. (2019a)
Mitochondria	Triphenylphosphine	Titanium dioxide-GNPs	18	MCF-7(4Gy)	Mitochondrial oxygen consumption rate↓	MCF-7 and 4T1 tumor bearing mice(6Gy)	- Scarce damages against helathy tissues – 100% survival - Removed tumor within 12(MCF-7) and 14(4T-1)cells	Li et al. (2018)
	CCYKFR peptide	Gold nanoclusters	2.7	MCF7(4Gy)	• Signals in the mitochondria by confocal laser scanning microscopy↑ • ROS↑	-	Sensitization enhancement ratio was 1.31	Fang et al. (2017)
	-	Hafnium–Rubidium metal organic framework	98.1 ± 4.1	MC38 (0–16Gy)	• Mitochondrial membrane potential↓ • Cytochrome *c* release to cytosol↑ • Caspase 3 protein↑ (BCL-2 was unchanged)	MC38 tumor bearing mice (1Gy)	Radiation enhancement factor for 10% survival of was 2.68 Tumor weigh of 0.23 ± 0.16g (versus 2.69 ± 0.42 for control)	Ni et al. (2018b)
	4-carboxybutyl triphenylphosphonium bromide	Gadolinium doped Titanium dioxide	20	MCF-7(4Gy)	• Mitochondrial membrane potential↓ • Caspase 3↑	MCF-7 bearing nude mice (6Gy)	Decreased tumor volume from 80 to 100 mm^3 to ∼ 0 mm^3	Chen et al. (2019b)

manner under 6 Gy (6 MeV) of radiation. In contrast, CuO (in MCF-7 cells) (Jiang et al., 2019) and gold sparks (in KB cells) (Ma et al., 2017a) persuade cells to stay in G or S phase. Notably, increasing the number of NPs within the cell would intensify the role of the NPs in cell cycle modification. Hence, utilizing targeted delivery has been suggested to enhance the G2/M ratio (Xu et al., 2012). It is worth noting that delivering drugs that are well-defined in modulating the cell cycle could be further added to the nanoparticle effects (Gao et al., 2020; Ma et al., 2021; Xiong et al., 2018). Treating cells with the mentioned drugs and keeping the cells in G2/M phase have shown higher trafficking of GNPs into cells, benefiting radiosensitization-mediated cell death (Cheng et al., 2019; Guo et al., 2021). Of note, drugs could intervene DSBs repair for an enhanced cellular death (Wilson III et al., 2021) Decorating NPs with targeting ligands would enhance the trafficking of NPs into G2/M arrested cells (Hu et al., 2016).

The synergistic effects of various therapies coupled with RT (similar to the discussed adjuvant therapy with drugs), such as in combination with photodynamic therapy (Xie et al., 2021), gas delivery (Liu et al., 2017) or immunotherapy (Ni et al., 2018a), shows promise for combating cancer (Spyratou et al., 2012). The combined effects of RT and photothermal therapy can be subdivided into tumour microenvironment manipulation and cellular event induction (Hu et al., 2020; Qu et al., 2021). Following the photothermal effect, cell cycle modulation is the most important feature affecting the radiosensitization outcome (Chen et al., 2019c; Li et al., 2015b). Additionally, the time interval between photothermal therapy and radiation therapy governs the cell cycle distribution. Namely, the cell population in G2 phase was highest at 24 h in human mouth epidermal carcinoma cells photothermally treated with core-shell alginate-coated iron oxide-gold NPs (Safari et al., 2020)

8. Organelle targeting by nanoradiosensitizers

Achieving effective cancer cell death with nanoradiosensitizers is highly correlated with their ability to overcome multiple barriers: (1) the cellular membrane, (2) endo/lysosomal degradation, (3) cytoplasmic transportation and (4) specific organelle destination. Therefore, the intracellular fate must be considered for increased effectiveness. The necessity to engineer nanoradiosensitizers to target a specific organelle is illustrated in Fig. 5.

8.1. Nanoradiosensitizers targeting the nucleus

The nucleus is the principal organelle that regulates vital cellular functions such as proliferation, growth and metabolism. In addition, the trafficking of enzymes, hormones and transcription factors through the

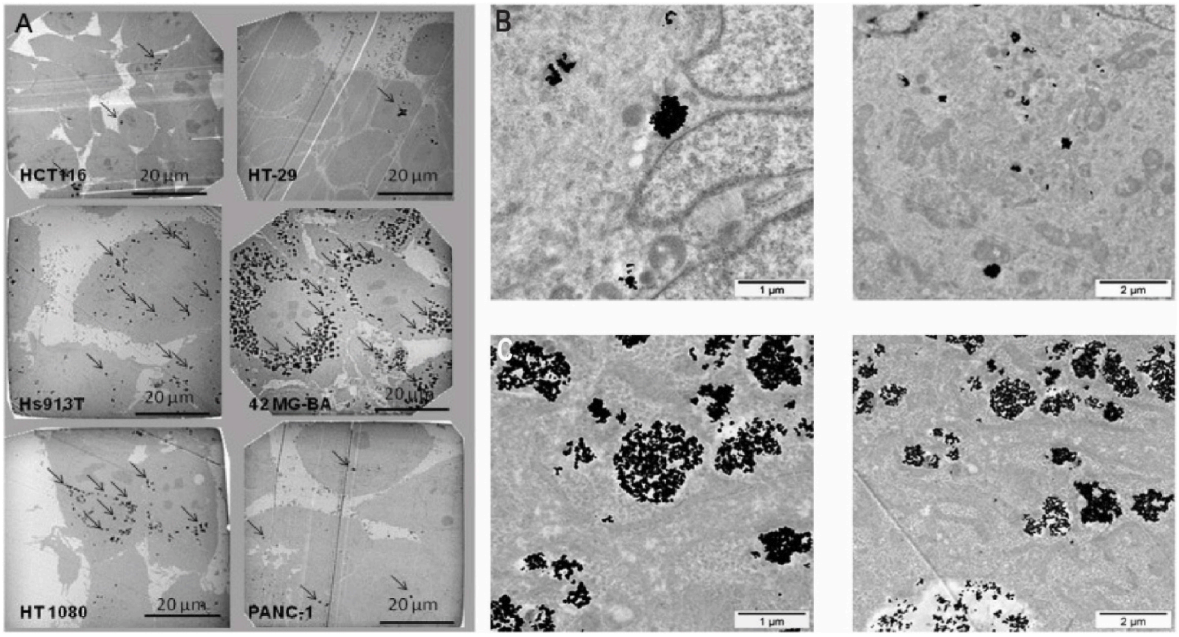

Fig. 3. A) TEM observations of the NBTXR3 subcellular distribution in HCTM116, HT-29, Hs913T, 42 MG-BA, HT1080 and PANC-1 cells. Cluster sizes in B) PANC-1 and C) 42-MG-BA cells. (Reproduced with permission from (Marill et al., 2014) Copyright Springer Nature.).

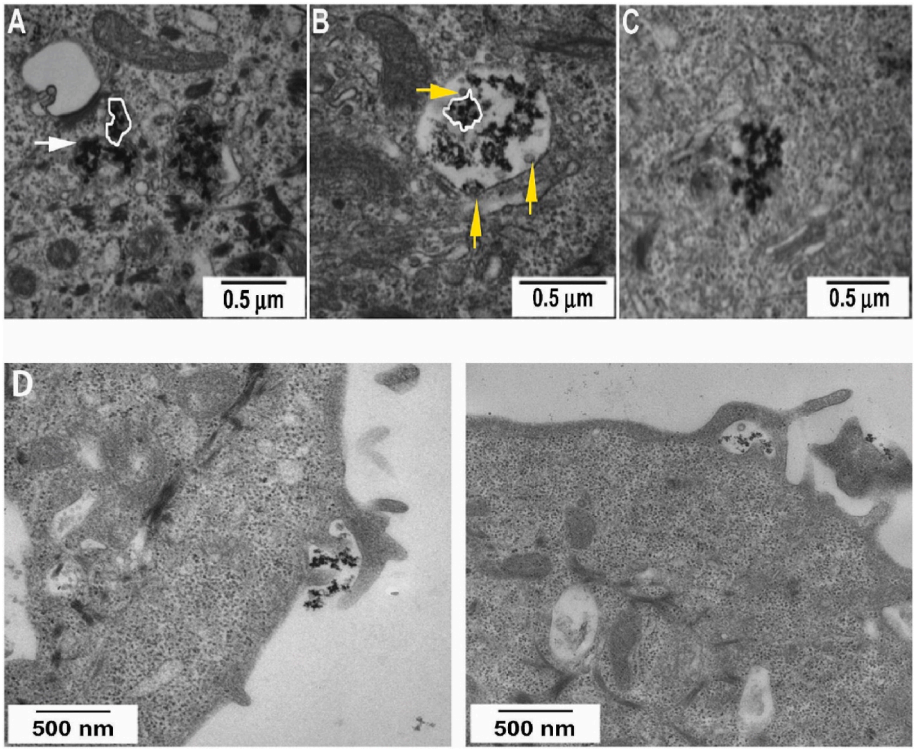

Fig. 4. A and B) TEM images of GdNP accumulation inside vacuoles and C) without a membrane. D) Macropinocytosis of GdNPs. (Reproduced with permission from (Rima et al., 2013) Copyright Elsevier.).

nuclear membrane is imperative for cell survival. Moreover, the DNA-dependent response of various therapeutic modalities has attracted the interest of researchers in the last two decades to increase the efficacy of therapies (Faustino et al., 2007). Namely, the anticancer response of some clinically approved drugs (e.g., cisplatin) is highly correlated with the quality of the interaction with DNA (Brabec et al., 2017). Initial efforts were driven by using viral/synthetic vectors and extracted plasmids to precisely translocate genes towards the nucleus (Faustino et al., 2007).

NP-induced DNA damage is a complex process that includes physical, chemical and biological factors. The success of radiation therapy is highly dependent on the type of lesion it causes. Three major DNA lesions are anticipated to interact with the produced ROS: single-strand breaks (SSBs), double-strand breaks (DSBs) and locally multiplied damaged sites. SSBs are the breakage of the one strands of the DNA backbone. Applying 1 Gy of radiation elicits approximately 1000 SSBs,

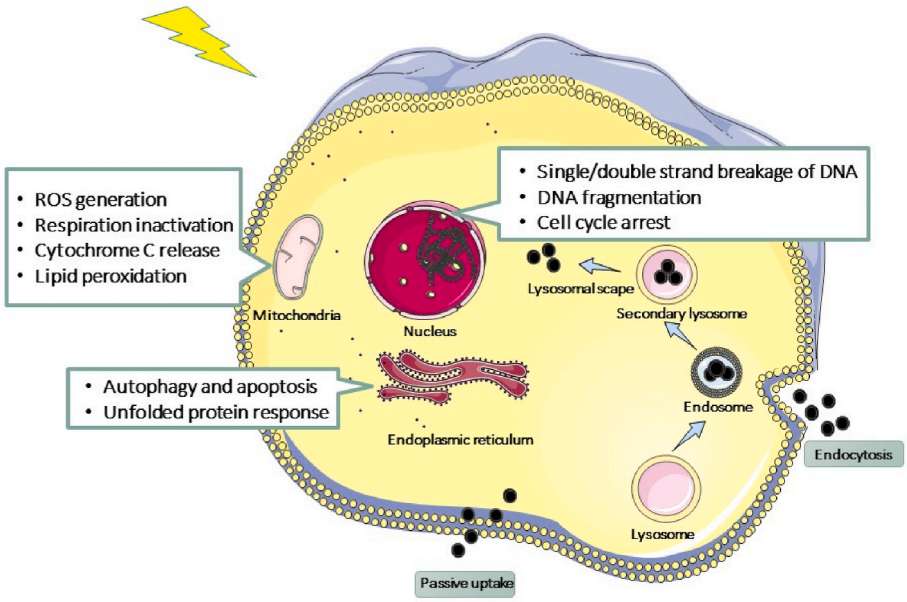

Fig. 5. Schematic overview of various intracellularly targeted radiosensitizers.

which are ultimately repaired by cellular processes; thus, this form of cell death has low efficacy. DSBs, which imply the breakage of both strands of the DNA backbone, have reduced repair by the cell repair system (Williams and Zhang, 2021; Yates, 2021). DSBs result in much more cell death and an increased number of DNA mutations; however, their therapeutic limiting factor is the low incidence of this type of breakage, causing on the order of 40 DSBs for each 1 Gy of irradiation. The last group, locally multiplied damaged sites, is associated with the concurrent incidence of DSBs and SSBs damage to a small number of bases. The complexity of the factors involved in this type of cell death needs more consideration for multimodal therapies such as photothermal/radiotherapy (Song et al., 2019), photothermal/photodynamic/radiotherapy (Guo et al., 2017; Xu et al., 2020) and photothermal/chemotherapy/radiotherapy(Wang et al., 2019b).

In comparison to cancer cells in the classic RT, which are mostly composed of low electron density molecules (mostly water, proteins), functionalized hafnium oxide nanoparticles (NBTXR3) have a higher probability of interacting with arriving ionizing radiation and depositing a higher energy dose within cancer cells because of their high electron density. Irradiation of high Z NPs and X-rays with an energy level that is the same or higher than the K-edge energy of the metallic material is very promising. In this manner, nanoradiosensitizers are irradiated at the same or higher K-edge energy as high-Z NPs, led to the Auger electrons generation by local release of K-shell electrons.

There have been clinical trials by Nanobiotix and NH TherAguix on hafnium oxide (NBTXR3, PEP503) and polysiloxane Gd-chelate(AGuiX), respectively. With regards to Table (3), NBTXR3 and AGuiX are passing several clinical trials on multiple type of cancers and various radiation-therapy methods. AGuiX is administered intravenously which implies the role of enhanced permeability and retention (EPR) effect in tumor accumulation (Lux et al., 2019). In comparison with the common clinical instructions, the utilized radiation dose in the nanoradiosensitizers at the same cancer types and radiation therapy method are lower (Cahlon et al., 2008). In phase II–III of NBTXR3, they could elicit two-fold higher pathological complete response in patients with soft-tissue sarcoma in comparison with radiation-only group (Bonvalot et al., 2019). However, some adverse effects (e.g., skin injury, stomatitis) are remained unsolved which demands more considerations (Bonvalot et al., 2019; Hoffmann et al., 2021).

Recently, several studies have described the role of gold NPs (GNPs) in suppressing cellular repair signals instead of causing direct or indirect DNA damage. Turnbull et al. (2019) observed similar $\gamma H2AX$ levels in GNP-treated (14 nm size, 6 nM) and nontreated S phase prostate cancer cell under γ rays(4 Gy), which indicates a negligible role of NPs in DNA DSBs. They evaluated the thymidylate synthase (TS) level as an essential enzyme in DNA homologous recombination repair following irradiation. Surprisingly, the TS level was downregulated after irradiation, which unveiled that the role of GNPs in cell death occurs by altering the cellular repair mechanism instead of causing DNA damage as previously reported.

To precisely study the biological effects by controlling the incident radiotherapy energy, which results in preservation of the physical properties of the NPs inside the cells, Ghita et al. (2017) used targeted X-ray microbeam irradiation (2 ± 0.2 Gy, 0.15 ± 0.015 Gy/s), which is capable of targeting the cytoplasm and nucleus separately. Considering the distance of the GNPs (1.9 nm size, 500 μg/mL) from the nucleus, they observed a high level of DNA abnormalities in cells when the microbeam was focused on the GNPs contained in the cytoplasm. This result emphasizes the biological or chemical role of radiotherapy in DNA structural damage.

8.1.1. *Active targeting of the nucleus*

The nucleus is surrounded by the nuclear envelope (NE), a bilayered membrane that isolates the nuclear space from the cytoplasm in eukaryotic cells. The NE bears ~ 60 nm channels named nuclear pore complexes (NPCs), which consist of ~ 30 types of nucleoporins (Nups), Moreover, a scaffold structure composed of Nups covers the interior part of the NPCs, which are responsible for stabilizing the membrane. On the other hand, the surface of the scaffolds is covered with abundant peripheral Nups that are enriched with phenylalanine-glycine (FG) (Rout et al., 2000). FG-Nups allow biomolecules of a certain size to permeate through the membrane, giving priority to those that are smaller (Popken et al., 2015). These proteins allow nuclear localization signal (NLS)-bound proteins to come in contact with karyopherins, which are soluble cellular receptor-carrying proteins (Macara, 2001). For instance, the T antigen of SV40 large T antigen (Kalderon et al., 1984) and a NLS from nucleoplasmin (Robbins et al., 1991) express protein sequences recognizable to karyopherins. Therefore, functionalization of larger NPs with NLS proteins facilitates nuclear targeting and internalization of the NPs in their active form.

8.1.1.1. Cell-penetrating peptides. A wide range of cell-penetrating

peptides (CPPs) are capable of penetrating the cell membrane. In recent decades, CPPs have been used to facilitate cargo delivery into cells (Kim et al., 2021). Generally, the various amino acids that constitute CPPs are subdivided into three major categories: cationic, amphipathic and hydrophobic (Milletti, 2012). In cationic CPPs, the presence of positively charged arginine and lysine residues initially mediates an electrostatic interaction with the cell membrane (Rothbard et al., 2004). Next, the guanidinium and ammonium functional groups of the arginine and lysine residues, respectively, form hydrogen bonds with phosphate groups for cell internalization (Rothbard et al., 2004). Penetratin, a 16 residue cationic CPP extracted from the Antennapedia homeodomain, has been widely investigated for nuclear targeting ability (Derossi et al., 1998). The electropositivity (Eiríksdóttir et al., 2010) and physical structure (Ohgita et al., 2020) of penetratin are the most important factors governing cell internalization. Amphipathic CPPs, also known as intermediate hydrophobic CPPs, interact with plasma membrane lipids to accelerate cellular uptake. Of note, an excessive number of hydrophobic residues on CPPs impede deep cell internalization (Walrant et al., 2012). Finally, hydrophobic CPPs are among the rarest CPPs and have been categorized as amphipathic. TP10 is analogous to transportin but with a removed initial N-terminus and diminished toxicity (Madani et al., 2011).

Nanoradiosensitizers entering lysosomes after endocytosis may have altered physicochemical properties, which diminishes their transport to the nucleus. In contrast, selective passive permeability across the cell membrane allows their direct introduction into the cytoplasm. CPPs are able to pass through the cell membrane via passive methods (Jones et al., 2005) and endocytotic methods with endo/lysosome escape capability (Hingorani et al., 2020). Recently, modification of NPs with CPPs, which results in direct transportation, has gained wide attention in the fields of imaging and therapy (Silva et al., 2019). CPPs are recruited for cargo delivery via their chemical or electrostatic bonding abilities (Kardani et al., 2019).

Feldherr et al. (Feldherr and Akin, 1990) coated GNPs with nucleoplasmin and assessed their passage through the NE. The cells were microinjected to overcome the membrane barrier and allow determination of the true number of NPs within the cytoplasm. The population of NPs inside the nucleus and cytoplasm varied as a function of NP size and the dividing/confluent status of the cells. To pass through the cell membrane and NE, Tkachenko et al. (2003) decorated NP surfaces with BSA and nucleus-targeting peptides. They reported that endosomal escape and cell uptake are both essential for reaching the nucleus. Thus, adjoining receptor-mediated endocytosis (RME) and NLS peptides in a single peptide fibre sequence can circumvent the endosomal pathway.

8.1.1.2. Polyarginine. As previously discussed, peptides possessing cationic charges due to the presence of arginine and lysine residues have favourable characteristics for passing through the cell membrane and targeting the nucleus. Arginine-containing peptides create a large number of hydrogen bonds with the lipid bilayer compared with lysine, which endows the arginine-rich peptides with enhanced internalization (Guterstam et al., 2009). In addition, multilamellar vesicle induction and fusion pore formation are recognized as passive mechanisms of internalization of nona-arginine (R9) (Allolio et al., 2018). It is worth noting that a minimum of 8 arginines are required for introduction into cells (Tünnemann et al., 2008).

In a recent study, Özçelik et al. (Ozcelik and Pratx, 2020) fabricated RGD/NLS-modified GNPs (10 μg/mL) that showed a 10% decrease in the surviving fraction of A549 cancer cells after treatment with 11.0 Gy of radiation compared to treatment with 7.1 Gy. The impact of GNP concentration and dosage on the surviving fraction of A549 cells was considerable. Aggregation of RGD/NLS/GNPs inside the nucleus was comparable to that of the bare GNPs with the NLS, which was structurally composed of a large number of lysine and arginine residues, presenting a high positive charge density. Yang et al. (2014) functionalized GNPs with RGD, NLS and a pentapeptide to overcome the cell membrane barrier, target the nucleus and withdraw protein corona formation.

Inspired by the positively charged characteristics of NLSs, similarly charged polymers were conjugated to NPs to target the nucleus (Ojea-Jiménez et al., 2012). In a study by Setua et al. (2014), polyethyleneimine-coated GNPs showed great repositioning near the nucleus in comparison with GNPs coated with a mercaptoundecanoic acid group, which led to an enhanced nanoradiosensitizing effect. Zhang et al. (2018a) functionalized gold NPs with octa-arginine (R8) and PEG simultaneously. The remarkable reduction in the survival ratio at various radiation dosages was correlated with the increased volume of produced ROS in the functionalized NP treatment group. There was no data regarding the role of R8-modified GNPs in cell nucleus targeting; however, time-dependent ≈5-fold cell internalization was found.

8.1.1.3. TAT peptide. The TAT peptide, derived from human immunodeficiency virus (HIV), is the major CPP that has been extensively studied for the intracellular delivery of cargos (Berry, 2008). TAT is composed of 13 amino acids (GRKKRRQRRRPPQ), and due to the presence of 6 arginine and 2 lysine residues, it is categorized as a cationic CPP (Kardani et al., 2019).

Hauser et al. (2016) conjugated TAT to dextran-coated Fe_3O_4 NPs to radiosensitize A549 cells. TAT permeabilized the lysosomes and directed the NPs towards the mitochondria/nucleus. Moreover, leveraging cell receptor-mediated endocytosis ligands and TAT-modified Fe_3O_4 showed promise to simultaneously circumvent the cell membrane and endolysosomes (He et al., 2015). The higher amount of ROS generated occurred as a result of the increased Fenton reaction upon iron ion release, which led to endolysosomal escape. Chang et al. (2017) synthesized a GNP/Si core/shell structure modified with RGD/CPP that enhanced ROS generation under radiation. Additionally, delivering nanoradiosensitizer drugs alongside nanoradiosensitizer NPs decorated with TAT effectively produces cancer cell death due to the combined effects (Fan et al., 2015b).

8.1.2. Passive diffusion into the nucleus

The passive diffusion of NPs across the nuclear membrane is under the control of Brownian motion within NPCs. Liang et al. (Huo et al., 2014) used diverse 2-, 6-, 10- and 16-nm tiopronin-modified GNPs to examine the effect of size on nuclear penetration. They observed that the number of 2 and 6 nm NPs in the nucleus was significantly higher than the number of 10 and 16 nm NPs inside the nucleus in a 24-h period. Lovrić et al. observed that smaller cadmium telluride (CdTe) quantum dots (QDs) (2.2 ± 0.1 nm) were present in greater numbers inside the nuclei of N9 cells than larger QDs (5.2 ± 0.1 nm) (Lovrić et al., 2005). In a study by Tang et al. (2014), the cell membrane and nuclear diffusion of three cadmium selenide (CdSe)/zinc sulfide (ZnS) QDs of various sizes (3, 4.8 and 8 nm) were studied. QDs with a size of 4.8 nm were more favoured for introduction into the cells; however, QDs with a size of only 3 nm were found in the nucleus. Huang et al. (2012) observed an increased amount of nuclear transportation for 2 and 6 nm GNPs, while 15 nm GNPs were localized within the cytoplasm of MCF-7 cells.

8.2. Lysosome targeting

Following the internalization inside the cells, the nanoparticles that reside in endosome are accumulated within lysosomes (Behzadi et al., 2017). Lysosomes are chiefly responsible for the degradation of proteins, polysaccharides, and complex lipids into amino acids (AAs), monosaccharides, and free fatty acid (Perera and Zoncu, 2016). Lysosomes contain over 60 distinct hydrolases, including lipases, proteases, and glycosidases. In order to ensure the activity of these enzymes, lysosome contains an acidic medium with pH ∼ 5. Adsorbed protein-based substances such as subcellular targeting moieties are prone to be degraded

in this stage (Wang et al., 2013b). Therefore, methods for disrupting the harsh medium of the lysosome is necessary to attain an efficient subcellular targeting. The endosomal escape of the nanoparticles is governed by the mechanism of through which they were taken up (Khalil et al., 2006; Rejman et al., 2005). The proton sponge effect intends that throughout acidification of the endosome, polymers with buffering capacity prevent the pH decline and cause the cell to keep pumping protons into the endosome in order to achieve the desired pH. This provokes an influx of chloride counterions and water molecules, which ultimately causes the endosomal rupture due to the increased pressure. Membrane fusion, swellable nanoparticles and membrane destabilization are the remained routes to escape from lysosome (Smith et al., 2018).

Most recently, research has focused on lysosome targeting for treating cancer (Iulianna et al., 2022). Targeting of the lysosome brings additional benefits for radiation therapy due to its role in radioresistance. The major known mechanisms by which the lysosome mediates radioresistance are assisting autophagy, up-regulation of cysteine cathepsin proteases, and activation of mammalian target of rapamycin (mTOR) (Zhang et al., 2018b). According to Jiang et al. (2020), radiosensitizers and photothermal agents derived from palladium (Pd) nanosheets were primarily accumulated within the lysosome, and their higher amount of generated ROS was associated with mitochondrial dysfunction, led to DNA DSBs. The Pd nanosheets were able to control the relative tumor size growth to 16, which was comparable to the control group (35 times). Pd nanosheets regulated the cell cycle phases by raising the proportion of G2/M in MCF-7 cells, hence improving cancer cell radiosensitivity. In addition, they represented high biocompatibility and photothermal conversion effect which shows promising for combination therapy of tumors.

8.3. Mitochondria-targeting nanoradiosensitizers

Mitochondria are the major energy-producing organelles in cells that generate ROS through oxidative phosphorylation as byproducts (Vakifahmetoglu-Norberg et al., 2017). ROS homeostasis governs the efficiency of radiosensitizing agents by balancing ROS quantity and antioxidant activity. Destabilization of the mitochondrial membrane following radiation evokes substantial ROS release and eventual DNA damage (McCann et al., 2021).

The outer membrane of the mitochondria is home to the Bcl-2 family of proteins, which are major regulators of internal cell death (Yamazaki et al., 2020). Notably, Bcl-2 prevents the mitochondrial permeability transition pore from releasing apoptotic factors inside cells (Cui et al., 2020). However, BAX and BAK, as Bcl-2 family members, form pores inside the mitochondrial membrane, leading to the release of a large amount of proapoptotic factors and cytochrome C into the cell (Ow et al., 2008; Reed et al., 1998). Notably, mitochondrial DNA is more prone to ionizing radiation damage than nuclear DNA (LeDoux et al., 1999).

Owing to the substantial effects of mitochondria during cancer cell death, several pharmaceutical agents that modulate mitochondrial processes are being translated into clinical therapies for cancer treatment (Ngoi et al., 2020). In addition, altering mitochondrial function addresses several radiotherapeutic hurdles that result in enhanced efficacy (Tang et al., 2018). For instance, Benej et al. (2018) utilized papaverine to inhibit mitochondrial complexes to enhance oxygenation and radiotherapy outcomes. Mitochondrial attack by nanoradiosensitizers is often followed by increased ROS levels (Howard et al., 2020). Similar to nucleus-targeted therapy, several compounds and proteins have been identified to target the mitochondria (Cho et al., 2020). Namely, triphenylphosphonium, used as a mitochondrial membrane potential probe for decades, has shown promise when conjugated with polymers (Marrache and Dhar, 2012).

8.4. Endoplasmic reticulum-targeted nanoradiosensitizers

The endoplasmic reticulum (ER) is the least studied subcellular compartment in terms of cancer therapy. Designing highly selective and low molecular weight organic probes for ER imagining faces challenges (McDonald et al., 2016). The ER controls the homeostasis of calcium ions and biosynthesis of lipids. Furthermore, approximately one-third of the intra/extracellular signalling proteins pass from the ER to their destination, and productive folding of NPs is performed in the ER (Ninagawa et al., 2020). Disruption of the protein folding function of the ER induces ER stress, which may cause cellular death. In eukaryotic cells, after sensing ER stress, cells respond through an adaptation named the unfolded protein response (UPR) (Ron and Walter, 2007). During the UPR, tumour cells have a higher survival ratio due to the hypoxic microenvironment, enhanced angiogenesis, increased aggressiveness and immunosuppressive effects (Cubillos-Ruiz et al., 2017).

The UPR drives cells into dormancy, which diminishes radiotherapy efficiency (Urra et al., 2016). Liu et al. (2019) induced the UPR by knocking down the protein disulfide isomerase (PDI) gene. Moreover, increased UPR activity restricts DNA repair ability and led to enhanced glioblastoma multiforme (GBM) death under IR. Of note, IR stimulates ER stress, which contributes to the production of multiple proteins (Walczak et al., 2019). Dadey et al. (2017) found that GBM and non–small cell lung cancer (NSCLC) radioresistance is associated with the protein GRP78, which was upregulated under ER stress. Referring to this IR-associated ER stress, they targeted GRP78 using an antibody that endowed higher radiation efficacy. Moreover, IR terminates cellular death directly by evolving ER stress through the protein kinase R (PKR)-like endoplasmic reticulum kinase (PERK) pathway (Dadey et al., 2018; Kim et al., 2010).

NP crosstalk with the ER has recently gained attention in cancer therapy (Cao et al., 2017). Yasui et al. synthesized PEGylated polyamine nanogels containing GNPs and assessed their radiosensitization effects on murine squamous carcinoma (SCCII), human lung adenocarcinoma (A549) and Chinese hamster (V79) cells. The NPs were distributed alongside the nuclear membrane and elicited delayed DNA DSBs repair after IR (200 keV) application. Elevated expression of inositol-requiring enzyme 1α (IRE1α) and phosphorylated PERK unveiled the role of the ER in augmenting the IR outcome.

9. Therapeutic effect of the intracellular targeting

As discussed before, the subcellular targeted nanoradiosensitizers are able to increase the cancer cell's death *in-vitro*. In *in-vivo* studies, inhibition of the tumor growth/decreasing the tumor's volume and avoiding the recurrence should be fulfilled by nanoradiosensitizers. Of note, the cytosolic distribution of the non-targeted nanoradiosensitizers are able to increase the DEF by spontaneously affecting of the organelles (McNamara et al., 2016). Table (4) shows the effect of the targeted radiosensitization using nanoradiosensitizers *in-vivo*.

10. Conclusion and future remarks

Classical radiotherapy has been thought to be revolutionized by the utilization of high-Z nanoradiosensitizers. Enhanced evaluations of the interactions of these structures with cells are crucial to achieving an improved outcome. Furthermore, guiding nanoradiosensitizers towards death-determining cellular compartments would considerably enhance the curative ratio. Additionally, choosing a specific size for radiosensitizer cell internalization is controversial; however, the literature strongly suggests a size of approximately 50 nm to be optimal for cell internalization and radiosensitization. NPs 100 nm in size undergo clathrin-mediated endocytosis; otherwise, the endocytotic pathway is followed based on NP size, cell type, etc. More considerations are needed when choosing an optimum shape for nanoradiosensitizers due to their role in increasing cellular uptake and directing towards a particular

endocytosis mechanism. Spherical, cube, rod and disk-shaped GNPs have shown high to low internalization ratios, respectively. Subcellular targeting of nanoradiosensitizers is the latest method being investigated to increase radiation therapy efficacy. However, further studies using novel instruments such as super-resolution microscopy and imaging flow cytometry are necessary to survey the exact mechanism of cell death after nanoradiosensitzer treatment.

Studies on cell-NP interactions are governed by multiple factors, and inexperience may mislead researchers. In addition, due to the distinct effects of each kind of therapy on cellular behaviour, the combined effects of multiple therapeutic modalities demand further cell-nanomaterial interaction studies. This may shed light on the neglected mechanism behind the synergistic effects of combination therapy and its further use in the clinic. In this way, the coadministration of docetaxel with nanoradiosensitizers causes the cell population to arrest in G2/M phase with the greatest radiation vulnerability and higher nanomaterial uptake(Cheng et al., 2019).

Emerging technologies, such as lab-on-chip and organoids, could be leveraged to provide deeper insight into cell-nanomaterial interactions at the tissue level owing to their similar physicochemical environments. These technologies could also provide information to study the patient-specific response prior to clinical radiation therapy. Undoubtedly, utilizing these new tools would accelerate nanoradiosensitizer translation into the clinic.

Targeting of the remaining non-studied organelles should be investigated individually or in combination. Also, there is an urgent need to develop additional straightforward peptides to enable precise mono- or multiple targeting. Biomimetic routes may be beneficial to synthesize a charge-resembling polymeric chain or engineered nanoradiosensitizer (e.g., size, charge) to recapitulate the peptidic features. The cell-nano interaction and intracellular localization was limited to specific morphology of nanoradiosensitizer (e.g. spherical, rod). Nowadays, by adventing of the new shape of high-z nanoradiosensitizers such as nanosheets, there is a demand for unravelling their interaction with the cancer cells.

The benefits of the organelle-targeting nanoradiosensitizer were not confirmed in any clinical trials. It makes sense to execute organelle-targeted radiosensitizer treatments in clinical settings in light of the animal studies that demonstrate a relatively low risk of injury to healthy tissues. Adverse effects were observed in the clinical trials of the nanoradiosensitizers. Intracellular targeting may tackle the unsolved radiation therapy adverse events and toxicities.

Radioresitance is one of the major hurdles to radiation therapy, which has a detrimental effect on the healthy tissues. Thus, targeting should not be limited to the localization, also the post-biochemical cascades that may induce radioresistance. For instance, endoplasmic reticulum stress followed by radiation therapy may induce radioresistancy, however, the nanosensitizer's role in controlling this cellular event is unknown. Epithelial-mesenchymal transition (EMT) is a principal route that induces metastatic cancers and plays a role as a radioresistance element (Dudás et al., 2020). This issue has been suggested by the EMT markers expressed by surviving cancer cells after RT (Zhou et al., 2020). Therefore, the long term follow-up of the survived cancer cells post nanoradiosensitizer treatment is necessary to study.

Declaration of competing interest

None.

References

Abbas, Z., Rehman, S., 2018. An overview of cancer treatment modalities. Neoplasma (Bratisl.) 1, 139–157.
Aderem, A., Underhill, D.M., 1999. Mechanisms of phagocytosis in macrophages. Annu. Rev. Immunol. 17, 593–623.
Ahmad, R., Schettino, G., Royle, G., Barry, M., Pankhurst, Q.A., Tillement, O., Russell, B., Ricketts, K., 2020. Radiobiological implications of nanoparticles following radiation treatment. Part. Part. Syst. Char. 37, 1900411.
Alhussan, A., Bozdoğan, E.P.D., Chithrani, D.B., 2021. Combining gold nanoparticles with other radiosensitizing agents for unlocking the full potential of cancer radiotherapy. Pharmaceutics 13, 442.
Alizadeh, M.J., Kariminezhad, H., Monfared, A.S., Mostafazadeh, A., Amani, H., Niksirat, F., Pourbagher, R., 2019. An experimental study about the application of Gadolinium oxide nanoparticles in magnetic theranostics. Mater. Res. Express 6, 065025.
Allolio, C., Magarkar, A., Jurkiewicz, P., Baxová, K., Javanainen, M., Mason, P.E., Šachl, R., Cebecauer, M., Hof, M., Horinek, D., 2018. Arginine-rich cell-penetrating peptides induce membrane multilamellarity and subsequently enter via formation of a fusion pore. Proc. Natl. Acad. Sci. USA 115, 11923–11928.
Anselmo, A.C., Mitragotri, S., 2016. Nanoparticles in the clinic. Bioeng. Transl. Med. 1, 10–29.
Arata, Y., Takagi, H., 2019. Quantitative studies for cell-division cycle control. Front. Physiol. 10, 1022.
Bae, G.D., Park, E.-Y., Kim, K., Jang, S.-E., Jun, H.-S., Oh, Y.S., 2019. Upregulation of caveolin-1 and its colocalization with cytokine receptors contributes to beta cell apoptosis. Sci. Rep. 9, 1–10.
Behzadi, S., Serpooshan, V., Tao, W., Hamaly, M.A., Alkawareek, M.Y., Dreaden, E.C., Brown, D., Alkilany, A.M., Farokhzad, O.C., Mahmoudi, M., 2017. Cellular uptake of nanoparticles: journey inside the cell. Chem. Soc. Rev. 46, 4218–4244.
Benej, M., Hong, X., Vibhute, S., Scott, S., Wu, J., Graves, E., Le, Q.-T., Koong, A.C., Giaccia, A.J., Yu, B., 2018. Papaverine and its derivatives radiosensitize solid tumors by inhibiting mitochondrial metabolism. Proc. Natl. Acad. Sci. USA 115, 10756–10761.
Berry, C., 2008. Intracellular Delivery of Nanoparticles via the HIV-1 Tat Peptide.
Bonvalot, S., Rutkowski, P.L., Thariat, J., Carrère, S., Ducassou, A., Sunyach, M.-P., Agoston, P., Hong, A., Mervoyer, A., Rastrelli, M., 2019. NBTXR3, a first-in-class radioenhancer hafnium oxide nanoparticle, plus radiotherapy versus radiotherapy alone in patients with locally advanced soft-tissue sarcoma (Act. In. Sarc): a multicentre, phase 2–3, randomised, controlled trial. Lancet Oncol. 20, 1148–1159.
Bouallegui, Y., Ben Younes, R., Turki, F., Mezni, A., Oueslati, R., 2018. Effect of exposure time, particle size and uptake pathways in immune cell lysosomal cytotoxicity of mussels exposed to silver nanoparticles. Drug Chem. Toxicol. 41, 169–174.
Brabec, V., Hrabina, O., Kasparkova, J., 2017. Cytotoxic platinum coordination compounds. DNA binding agents. Coord. Chem. Rev. 351, 2–31.
Bridot, J.-L., Faure, A.-C., Laurent, S., Riviere, C., Billotey, C., Hiba, B., Janier, M., Josserand, V., Coll, J.-L., Vander Elst, L., 2007. Hybrid gadolinium oxide nanoparticles: multimodal contrast agents for in vivo imaging. J. Am. Chem. Soc. 129, 5076–5084.
Bromma, K., Rieck, K., Kulkarni, J., O'Sullivan, C., Sung, W., Cullis, P., Schuemann, J., Chithrani, D.B., 2019. Use of a lipid nanoparticle system as a Trojan horse in delivery of gold nanoparticles to human breast cancer cells for improved outcomes in radiation therapy. Cancer Nanotechnol. 10, 1.
Brun, E., Sanche, L., Sicard-Roselli, C., 2009. Parameters governing gold nanoparticle X-ray radiosensitization of DNA in solution. Colloids Surf., B: Biointerfaces 72, 128–134.
Butterworth, K., Coulter, J., Jain, S., Forker, J., McMahon, S., Schettino, G., Prise, K., Currell, F., Hirst, D., 2010. Evaluation of cytotoxicity and radiation enhancement using 1.9 nm gold particles: potential application for cancer therapy. Nanotechnology 21, 295101.
Cahlon, O., Zelefsky, M.J., Shippy, A., Chan, H., Fuks, Z., Yamada, Y., Hunt, M., Greenstein, S., Amols, H., 2008. Ultra-high dose (86.4 Gy) IMRT for localized prostate cancer: toxicity and biochemical outcomes. Int. J. Radiat. Oncol. Biol. Phys. 71, 330–337.
Cai, Z., Pignol, J.P., Chattopadhyay, N., Kwon, Y.L., Lechtman, E., Reilly, R.M., 2013. Investigation of the effects of cell model and subcellular location of gold nanoparticles on nuclear dose enhancement factors using Monte Carlo simulation. Med. Phys. 40, 114101.
Cao, Y., Long, J., Liu, L., He, T., Jiang, L., Zhao, C., Li, Z., 2017. A review of endoplasmic reticulum (ER) stress and nanoparticle (NP) exposure,. Life Sci. 186, 33–42.
Chang, Y., He, L., Li, Z., Zeng, L., Song, Z., Li, P., Chan, L., You, Y., Yu, X.-F., Chu, P.K., 2017. Designing core–shell gold and selenium nanocomposites for cancer radiochemotherapy. ACS Nano 11, 4848–4858.
Chen, F., Zhang, X.H., Hu, X.D., Liu, P.D., Zhang, H.Q., 2018. The effects of combined selenium nanoparticles and radiation therapy on breast cancer cells in vitro. Artific. Cell. Nanomed. Biotechnol. 46, 937–948.
Chen, X., Song, J., Chen, X., Yang, H., 2019a. X-ray-activated nanosystems for theranostic applications. Chem. Soc. Rev. 48, 3073–3101.
Chen, Y., Li, N., Wang, J., Zhang, X., Pan, W., Yu, L., Tang, B., 2019b. Enhancement of mitochondrial ROS accumulation and radiotherapeutic efficacy using a Gd-doped titania nanosensitizer. Theranostics 9, 167.
Chen, Y., Zhao, G., Wang, S., He, Y., Han, S., Du, C., Li, S., Fan, Z., Wang, C., Wang, J., 2019c. Platelet-membrane-camouflaged bismuth sulfide nanorods for synergistic radio-photothermal therapy against cancer. Biomater. Sci. 7, 3450–3459.
Cheng, X., Zhang, X., Liu, P., Xia, L.-Y., Jiang, Y.-W., Gao, G., Wang, H.-Y., Li, Y.-H., Ma, N., Ran, H.-H., 2019. Sequential treatment of cell cycle regulator and nanoradiosensitizer achieves enhanced radiotherapeutic outcome. ACS Appl. Bio Mater. 2, 2050–2059.
Chithrani, B.D., Chan, W.C., 2007. Elucidating the mechanism of cellular uptake and removal of protein-coated gold nanoparticles of different sizes and shapes. Nano Lett. 7, 1542–1550.

Chithrani, B.D., Ghazani, A.A., Chan, W.C., 2006. Determining the size and shape dependence of gold nanoparticle uptake into mammalian cells. Nano Lett. 6, 662–668.
Chithrani, D.B., Jelveh, S., Jalali, F., van Prooijen, M., Allen, C., Bristow, R.G., Hill, R.P., Jaffray, D.A., 2010. Gold nanoparticles as radiation sensitizers in cancer therapy. Radiat. Res. 173, 719–728.
Cho, H., Cho, Y.-Y., Shim, M.S., Lee, J.Y., Lee, H.S., Kang, H.C., 2020. Mitochondria-targeted drug delivery in cancers. Biochim. Biophys. Acta, Mol. Basis Dis., 165808
Choi, J.W., Moon, W.-J., 2019. Gadolinium deposition in the brain: current updates. Korean J. Radiol. 20, 134–147.
Choo, P., Liu, T., Odom, T.W., 2021. Nanoparticle shape determines dynamics of targeting nanoconstructs on cell membranes. J. Am. Chem. Soc. 143 (12), 4550–4555.
Cluntun, A.A., Lukey, M.J., Cerione, R.A., Locasale, J.W., 2017. Glutamine metabolism in cancer: understanding the heterogeneity. Trends in cancer 3, 169–180.
Cong, V.T., Wang, W., Tilley, R.D., Sharbeen, G., Phillips, P.A., Gaus, K., Gooding, J.J., 2021. Can the shape of nanoparticles enable the targeting to cancer cells over healthy cells? Adv. Funct. Mater., 2007880
Contini, C., Schneemilch, M., Gaisford, S., Quirke, N., 2018. Nanoparticle–membrane interactions. J. Exp. Nanosci. 13, 62–81.
Coulter, J.A., Jain, S., Butterworth, K.T., Taggart, L.E., Dickson, G.R., McMahon, S.J., Hyland, W.B., Muir, M.F., Trainor, C., Hounsell, A.R., 2012. Cell type-dependent uptake, localization, and cytotoxicity of 1.9 nm gold nanoparticles. Int. J. Nanomed. 7, 2673.
Cubillos-Ruiz, J.R., Bettigole, S.E., Glimcher, L.H., 2017. Tumorigenic and immunosuppressive effects of endoplasmic reticulum stress in cancer. Cell 168, 692–706.
Cui, L., Tse, K., Zahedi, P., Harding, S.M., Zafarana, G., Jaffray, D.A., Bristow, R.G., Allen, C., 2014. Hypoxia and cellular localization influence the radiosensitizing effect of gold nanoparticles (AuNPs) in breast cancer cells. Radiat. Res. 182, 475–488.
Cui, Y., Pan, M., Ma, J., Song, X., Cao, W., Zhang, P., 2020. Recent progress in the use of mitochondrial membrane permeability transition pore in mitochondrial dysfunction-related disease therapies. Mol. Cell. Biochem. 1–14.
Dadey, D.Y., Kapoor, V., Hoye, K., Khudanyan, A., Collins, A., Thotala, D., Hallahan, D. E., 2017. Antibody targeting GRP78 enhances the efficacy of radiation therapy in human glioblastoma and non–small cell lung cancer cell lines and tumor models. Clin. Cancer Res. 23, 2556–2564.
Dadey, D.Y., Kapoor, V., Khudanyan, A., Thotala, D., Hallahan, D.E., 2018. PERK regulates glioblastoma sensitivity to ER stress although promoting radiation resistance. Mol. Cancer Res. 16, 1447–1453.
Damm, E.-M., Pelkmans, L., Kartenbeck, J.r., Mezzacasa, A., Kurzchalia, T., Helenius, A., 2005. Clathrin-and caveolin-1–independent endocytosis: entry of simian virus 40 into cells devoid of caveolae. J. Cell Biol. 168, 477–488.
Delorme, R., Taupin, F., Flaender, M., Ravanat, J.L., Champion, C., Agelou, M., Elleaume, H., 2017. Comparison of gadolinium nanoparticles and molecular contrast agents for radiation therapy-enhancement. Med. Phys. 44, 5949–5960.
Derossi, D., Chassaing, G., Prochiantz, A., 1998. Trojan peptides: the penetratin system for intracellular delivery. Trends Cell Biol. 8, 84–87.
Detappe, A., Kunjachan, S., Rottmann, J., Robar, J., Tsiamas, P., Korideck, H., Tillement, O., Berbeco, R., 2015. AGuIX nanoparticles as a promising platform for image-guided radiation therapy. Cancer Nanotechnol. 6, 1–9.
Detappe, A., Kunjachan, S., Sancey, L., Motto-Ros, V., Biancur, D., Drane, P., Guieze, R., Makrigiorgos, G.M., Tillement, O., Langer, R., 2016. Advanced multimodal nanoparticles delay tumor progression with clinical radiation therapy. J. Contr. Release 238, 103–113.
Detappe, A., Thomas, E., Tibbitt, M.W., Kunjachan, S., Zavidij, O., Parnandi, N., Reznichenko, E., Lux, F., Tillement, O., Berbeco, R., 2017. Ultrasmall silica-based bismuth gadolinium nanoparticles for dual magnetic resonance–computed tomography image guided radiation therapy. Nano Lett. 17, 1733–1740.
Dini, L., Panzarini, E., Serra, A., Buccolieri, A., Manno, D., 2011. Synthesis and in vitro cytotoxicity of glycans-capped silver nanoparticles. Nanomater. Nanotechnol. 1, 10.
Donahue, N.D., Acar, H., Wilhelm, S., 2019. Concepts of nanoparticle cellular uptake, intracellular trafficking, and kinetics in nanomedicine. Adv. Drug Deliv. Rev. 143, 68–96.
Dudás, J., Ladányi, A., Ingruber, J., Steinbichler, T.B., Riechelmann, H., 2020. Epithelial to mesenchymal transition: a mechanism that fuels cancer radio/chemoresistance,. Cells 9, 428.
Dufort, S., Bianchi, A., Henry, M., Lux, F., Le Duc, G., Josserand, V., Louis, C., Perriat, P., Crémillieux, Y., Tillement, O., 2015. Nebulized gadolinium-based nanoparticles: a theranostic approach for lung tumor imaging and radiosensitization. Small 11, 215–221.
Dufort, S., Le Duc, G., Salomé, M., Bentivegna, V., Sancey, L., Bräuer-Krisch, E., Requardt, H., Lux, F., Coll, J.-L., Perriat, P., 2016. The high radiosensitizing efficiency of a trace of gadolinium-based nanoparticles in tumors,. Sci. Rep. 6, 1–8.
Ehrlich, M., Boll, W., Van Oijen, A., Hariharan, R., Chandran, K., Nibert, M.L., Kirchhausen, T., 2004. Endocytosis by random initiation and stabilization of clathrin-coated pits. Cell 118, 591–605.
Eiríksdóttir, E., Konate, K., Langel, Ü., Divita, G., Deshayes, S., 2010. Secondary structure of cell-penetrating peptides controls membrane interaction and insertion. Biochim. Biophys. Acta Biomembr. 1798, 1119–1128.
Fan, W., Shen, B., Bu, W., Zheng, X., He, Q., Cui, Z., Ni, D., Zhao, K., Zhang, S., Shi, J., 2015a. Intranuclear biophotonics by smart design of nuclear-targeting photo-/radio-sensitizers co-loaded upconversion nanoparticles. Biomaterials 69, 89–98.
Fan, W., Shen, B., Bu, W., Zheng, X., He, Q., Cui, Z., Zhao, K., Zhang, S., Shi, J., 2015b. Design of an intelligent sub-50 nm nuclear-targeting nanotheranostic system for imaging guided intranuclear radiosensitization. Chem. Sci. 6, 1747–1753.
Fang, X., Wang, Y., Ma, X., Li, Y., Zhang, Z., Xiao, Z., Liu, L., Gao, X., Liu, J., 2017. Mitochondria-targeting Au nanoclusters enhance radiosensitivity of cancer cells. J. Mater. Chem. B 5, 4190–4197.
Faustino, R., Nelson, T., Terzic, A., Perez-Terzic, C., 2007. Nuclear transport: target for therapy. Clin. Pharmacol. Therapeut. 81, 880–886.
Feldherr, C.M., Akin, D., 1990. The permeability of the nuclear envelope in dividing and nondividing cell cultures,. J. Cell Biol. 111, 1–8.
Gao, S., Zhang, W., Wang, R., Hopkins, S.P., Spagnoli, J.C., Racin, M., Bai, L., Li, L., Jiang, W., Yang, X., 2020. Nanoparticles encapsulating nitrosylated maytansine to enhance radiation therapy. ACS Nano.
Geng, F., Song, K., Xing, J.Z., Yuan, C., Yan, S., Yang, Q., Chen, J., Kong, B., 2011. Thio-glucose bound gold nanoparticles enhance radio-cytotoxic targeting of ovarian cancer. Nanotechnology 22, 285101.
Geng, F., Xing, J.Z., Chen, J., Yang, R., Hao, Y., Song, K., Kong, B., 2014. Pegylated glucose gold nanoparticles for improved in-vivo bio-distribution and enhanced radiotherapy on cervical cancer. J. Biomed. Nanotechnol. 10, 1205–1216.
Gheran, C.V., Voicu, S.N., Rigaux, G., Callewaert, M., Chuburu, F., Dinischiotu, A., 2017. Biological effects induced by Gadolinium nanoparticles on Lymphocyte A20 cell line. EuroBiotech. J. 1, 57–64.
Ghita, M., McMahon, S.J., Taggart, L.E., Butterworth, K.T., Schettino, G., Prise, K.M., 2017. A mechanistic study of gold nanoparticle radiosensitisation using targeted microbeam irradiation,. Sci. Rep. 7, 1–12.
Giocanti, N., Hennequin, C., Balosso, J., Mahler, M., Favaudon, V., 1993. DNA repair and cell cycle interactions in radiation sensitization by the topoisomerase II poison etoposide. Cancer Res. 53, 2105–2111.
Goetz, J.G., Lajoie, P., Wiseman, S.M., Nabi, I.R., 2008. Caveolin-1 in tumor progression: the good, the bad and the ugly. Cancer Metastasis Rev. 27, 715–735.
Guidelli, E.J., Baffa, O., 2014. Influence of photon beam energy on the dose enhancement factor caused by gold and silver nanoparticles: an experimental approach. Med. Phys. 41, 032101.
Guo, X.-x., Guo, Z.-h., Wu, M., Lu, J.-s., Xie, W.-s., Zhong, Q.-z., Chi, Y.-j., Sun, X.-d., Wang, X.-m., Wang, J.-y., 2021. All-purpose nanostrategy based on dose deposition enhancement, cell cycle arrest. DNA Damage and ROS Production as Prostate Cancer Radiosensitizer for Potential Clinical Translation.
Guo, Z., Zhu, S., Yong, Y., Zhang, X., Dong, X., Du, J., Xie, J., Wang, Q., Gu, Z., Zhao, Y., 2017. Synthesis of BSA-coated BiOI@ Bi2S3 semiconductor heterojunction nanoparticles and their applications for radio/photodynamic/photothermal synergistic therapy of tumor. Adv. Mater. 29, 1704136.
Gustafson, H.H., Holt-Casper, D., Grainger, D.W., Ghandehari, H., 2015. Nanoparticle uptake: the phagocyte problem. Nano Today 10, 487–510.
Guterstam, P., Madani, F., Hirose, H., Takeuchi, T., Futaki, S., Andaloussi, S.E., Gräslund, A., Langel, Ü., 2009. Elucidating cell-penetrating peptide mechanisms of action for membrane interaction, cellular uptake, and translocation utilizing the hydrophobic counter-anion pyrenebutyrate. Biochim. Biophys. Acta Biomembr. 1788, 2509–2517.
Hanahan, D., Weinberg, R.A., 2000. The hallmarks of cancer. Cell 100, 57–70.
Hao, X., Wu, J., Shan, Y., Cai, M., Shang, X., Jiang, J., Wang, H., 2012. Caveolae-mediated endocytosis of biocompatible gold nanoparticles in living Hela cells. J. Phys.: Condensed Matter 24, 164207.
Hauser, A.K., Mitov, M.I., Daley, E.F., McGarry, R.C., Anderson, K.W., Hilt, J.Z., 2016. Targeted iron oxide nanoparticles for the enhancement of radiation therapy. Biomaterials 105, 127–135.
He, L., Lai, H., Chen, T., 2015. Dual-function nanosystem for synergetic cancer chemo-/radiotherapy through ROS-mediated signaling pathways. Biomaterials 51, 30–42.
Hemmer, E., Yamano, T., Kishimoto, H., Venkatachalam, N., Hyodo, H., Soga, K., 2013. Cytotoxic aspects of gadolinium oxide nanostructures for up-conversion and NIR bioimaging. Acta Biomater. 9, 4734–4743.
Hingorani, D.V., Crisp, J.L., Doan, M.K., Camargo, M.F., Quraishi, M.A., Aguilera, J., Gilardi, M., Gross, L.A., Jiang, T., Li, W.T., 2020. Redirecting extracellular proteases to molecularly guide radiosensitizing drugs to tumors. Biomaterials, 120032.
Ho, W., Gao, M., Li, F., Li, Z., Zhang, X.Q., Xu, X., 2021. Next-generation vaccines: nanoparticle-mediated DNA and mRNA delivery. Adv. Healthc. Mater. 10, 2001812.
Hoffmann, C., Calugaru, V., Borcoman, E., Moreno, V., Calvo, E., Liem, X., Salas, S., Doger, B., Jouffroy, T., Mirabel, X., 2021. Phase I dose-escalation study of NBTXR3 activated by intensity-modulated radiation therapy in elderly patients with locally advanced squamous cell carcinoma of the oral cavity or oropharynx. Eur. J. Cancer 146, 135–144.
Hoshyar, N., Gray, S., Han, H., Bao, G., 2016. The effect of nanoparticle size on in vivo pharmacokinetics and cellular interaction,. Nanomedicine 11, 673–692.
Hossain, M., Su, M., 2012. Nanoparticle location and material-dependent dose enhancement in X-ray radiation therapy. J. Phys. Chem. C 116, 23047–23052.
Howard, D., Sebastian, S., Le, Q.V.-C., Thierry, B., Kempson, I., 2020. Chemical mechanisms of nanoparticle radiosensitization and radioprotection: a review of structure-function relationships influencing reactive oxygen species,. Int. J. Mol. Sci. 21, 579.
Hu, G., Cun, X., Ruan, S., Shi, K., Wang, Y., Kuang, Q., Hu, C., Xiao, W., He, Q., Gao, H., 2016. Utilizing G2/M retention effect to enhance tumor accumulation of active targeting nanoparticles. Sci. Rep. 6, 1–10.
Hu, P., Zhang, X., Li, Y., Pichan, C., Chen, Z., 2018. Molecular interactions between silver nanoparticles and model cell membranes. Top. Catal. 61, 1148–1162.
Hu, Q., Huang, Z., Duan, Y., Fu, Z., Liu, B., 2020. Reprogramming tumor microenvironment with photothermal therapy. Bioconjugate Chem. 31, 1268–1278.

Huang, K., Ma, H., Liu, J., Huo, S., Kumar, A., Wei, T., Zhang, X., Jin, S., Gan, Y., Wang, P.C., 2012. Size-dependent localization and penetration of ultrasmall gold nanoparticles in cancer cells, multicellular spheroids, and tumors in vivo. ACS Nano 6, 4483–4493.

Huo, S., Jin, S., Ma, X., Xue, X., Yang, K., Kumar, A., Wang, P.C., Zhang, J., Hu, Z., Liang, X.-J., 2014. Ultrasmall gold nanoparticles as carriers for nucleus-based gene therapy due to size-dependent nuclear entry. ACS Nano 8, 5852–5862.

Iulianna, T., Kuldeep, N., Eric, F., 2022. The Achilles' heel of cancer: targeting tumors via lysosome-induced immunogenic cell death,. Cell Death Dis. 13, 1–10.

Jain, S., Coulter, J.A., Butterworth, K.T., Hounsell, A.R., McMahon, S.J., Hyland, W.B., Muir, M.F., Dickson, G.R., Prise, K.M., Currell, F.J., 2014. Gold nanoparticle cellular uptake, toxicity and radiosensitisation in hypoxic conditions. Radiother. Oncol. 110, 342–347.

Jain, S., Coulter, J.A., Hounsell, A.R., Butterworth, K.T., McMahon, S.J., Hyland, W.B., Muir, M.F., Dickson, G.R., Prise, K.M., Currell, F.J., 2011. Cell-specific radiosensitization by gold nanoparticles at megavoltage radiation energies. Int. J. Radiat. Oncol. Biol. Phys. 79, 531–539.

Jiang, Y.-W., Gao, G., Jia, H.-R., Zhang, X., Cheng, X., Wang, H.-Y., Liu, P., Wu, F.-G., 2020. Palladium nanosheets as safe radiosensitizers for radiotherapy. Langmuir 36, 11637–11644.

Jiang, Y.-W., Gao, G., Jia, H.-R., Zhang, X., Zhao, J., Ma, N., Liu, J.-B., Liu, P., Wu, F.-G., 2019. Copper oxide nanoparticles induce enhanced radiosensitizing effect via destructive autophagy. ACS Biomater. Sci. Eng. 5, 1569–1579.

Jokerst, J.V., Lobovkina, T., Zare, R.N., Gambhir, S.S., 2011. Nanoparticle PEGylation for imaging and therapy. Nanomedicine 6, 715–728.

Jones, S.W., Christison, R., Bundell, K., Voyce, C.J., Brockbank, S.M., Newham, P., Lindsay, M.A., 2005. Characterisation of cell-penetrating peptide-mediated peptide delivery. Br. J. Pharmacol. 145, 1093.

Kalderon, D., Richardson, W.D., Markham, A.F., Smith, A.E., 1984. Sequence requirements for nuclear location of simian virus 40 large-T antigen. Nature 311, 33–38.

Kamińska, I., Fronc, K., Sikora, B., Mouawad, M., Siemiarczuk, A., Szewczyk, M., Sobczak, K., Wojciechowski, T., Zaleszczyk, W., Minikayev, R., 2015. Upconverting/magnetic: Gd 2 O 3:(Er 3+, Yb 3+, Zn 2+) nanoparticles for biological applications: effect of Zn 2+ doping. RSC Adv. 5, 78361–78373.

Kao, H.-W., Lin, Y.-Y., Chen, C.-C., Chi, K.-H., Tien, D.-C., Hsia, C.-C., Lin, W.-J., Chen, F.-D., Lin, M.-H., Wang, H.-E., 2014. Biological characterization of cetuximab-conjugated gold nanoparticles in a tumor animal model. Nanotechnology 25, 295102.

Kardani, K., Milani, A., Shabani, H., S, Bolhassani, A., 2019. Cell penetrating peptides: the potent multi-cargo intracellular carriers,. Expet Opin. Drug Deliv. 16, 1227–1258.

Karimi, M., Ghasemi, A., Zangabad, P.S., Rahighi, R., Basri, S.M.M., Mirshekari, H., Amiri, M., Pishabad, Z.S., Aslani, A., Bozorgomid, M., 2016. Smart micro/nanoparticles in stimulus-responsive drug/gene delivery systems. Chem. Soc. Rev. 45, 1457–1501.

Karimi, S., Moshaii, A., Abbasian, S., Nikkhah, M., 2019. Surface plasmon resonance in small gold nanoparticles: introducing a size-dependent plasma frequency for nanoparticles in quantum regime. Plasmonics 14, 851–860.

Kaur, H., Pujari, G., Semwal, M.K., Sarma, A., Avasthi, D.K., 2013. In vitro studies on radiosensitization effect of glucose capped gold nanoparticles in photon and ion irradiation of HeLa cells. Nucl. Instrum. Methods Phys. Res. Sect. B: Beam Interact. Mater. Atoms 301, 7–11.

Kefayat, A., Ghahremani, F., Motaghi, H., Mehrgardi, M.A., 2019. Investigation of different targeting decorations effect on the radiosensitizing efficacy of albumin-stabilized gold nanoparticles for breast cancer radiation therapy. Eur. J. Pharmaceut. Sci. 130, 225–233.

Kempson, I., 2021. Mechanisms of nanoparticle radiosensitization. Wiley Interdiscip. Rev.: Nanomed. Nanobiotechnol. 13, e1656.

Khalil, I.A., Kogure, K., Futaki, S., Harashima, H., 2006. High density of octaarginine stimulates macropinocytosis leading to efficient intracellular trafficking for gene expression. J. Biol. Chem. 281, 3544–3551.

Khoshgard, K., Hashemi, B., Arbabi, A., Rasaee, M.J., Soleimani, M., 2014. Radiosensitization effect of folate-conjugated gold nanoparticles on HeLa cancer cells under orthovoltage superficial radiotherapy techniques. Phys. Med. Biol. 59, 2249.

Kim, G.C., Cheon, D.H., Lee, Y., 2021. Challenge to overcome current limitations of cell-penetrating peptides. Biochim. Biophys. Acta, Proteins Proteomics, 140604.

Kim, J.A., Åberg, C., Salvati, A., Dawson, K.A., 2012. Role of cell cycle on the cellular uptake and dilution of nanoparticles in a cell population. Nat. Nanotechnol. 7, 62.

Kim, K.W., Moretti, L., Mitchell, L.R., Jung, D.K., Lu, B., 2010. Endoplasmic reticulum stress mediates radiation-induced autophagy by perk-eIF2α in caspase-3/7-deficient cells. Oncogene 29, 3241–3251.

Kong, T., Zeng, J., Wang, X., Yang, X., Yang, J., McQuarrie, S., McEwan, A., Roa, W., Chen, J., Xing, J.Z., 2008. Enhancement of radiation cytotoxicity in breast-cancer cells by localized attachment of gold nanoparticles. Small 4, 1537–1543.

Korman, D., Ostrovskaya, L., Kuz'min, V., 2019. Induction of oxidative stress in tumor cells: a new strategy for drug therapy of malignant tumors,. Biophysics 64, 431–439.

Kryza, D., Taleb, J., Janier, M., Marmuse, L., Miladi, I., Bonazza, P., Louis, C., Perriat, P., Roux, S., Tillement, O., 2011. Biodistribution study of nanometric hybrid gadolinium oxide particles as a multimodal SPECT/MR/optical imaging and theragnostic agent. Bioconjugate Chem. 22, 1145–1152.

Kuczler, M.D., Olseen, A.M., Pienta, K.J., Amend, S.R., 2021. ROS-induced cell cycle arrest as a mechanism of resistance in polyaneuploid cancer cells (PACCs). Prog. Biophys. Mol. Biol.

Kuhn, D.A., Vanhecke, D., Michen, B., Blank, F., Gehr, P., Petri-Fink, A., Rothen-Rutishauser, B., 2014. Different endocytotic uptake mechanisms for nanoparticles in epithelial cells and macrophages. Beilstein J. Nanotechnol. 5, 1625–1636.

Kulkarni, S.A., Feng, S.-S., 2013. Effects of particle size and surface modification on cellular uptake and biodistribution of polymeric nanoparticles for drug delivery. Pharmaceut. Res. 30, 2512–2522.

Labbaf, S., Tsigkou, O., Müller, K.H., Stevens, M.M., Porter, A.E., Jones, J.R., 2011. Spherical bioactive glass particles and their interaction with human mesenchymal stem cells in vitro. Biomaterials 32, 1010–1018.

Le Lay, S., Kurzchalia, T.V., 2005. Getting rid of caveolins: phenotypes of caveolin-deficient animals. Biochim. Biophys. Acta Mol. Cell Res. 1746, 322–333.

LeDoux, S.P., Driggers, W.J., Hollensworth, B.S., Wilson, G.L., 1999. Repair of alkylation and oxidative damage in mitochondrial DNA, Mutation research. DNA Repair 434, 149–159.

Lee, C.-L., Blum, J.M., Kirsch, D.G., 2013. Role of p53 in regulating tissue response to radiation by mechanisms independent of apoptosis. Transl. Cancer Res. 2, 412.

Lee, E., Knecht, D.A., 2002. Visualization of actin dynamics during macropinocytosis and exocytosis. Traffic 3, 186–192.

Li, F., Li, Z., Jin, X., Liu, Y., Zhang, P., Li, P., Shen, Z., Wu, A., Chen, W., Li, Q., 2019. Ultra-small gadolinium oxide nanocrystal sensitization of non-small-cell lung cancer cells toward X-ray irradiation by promoting cytostatic autophagy. Int. J. Nanomed. 14, 2415.

Li, J., Lyv, Z., Li, Y., Liu, H., Wang, J., Zhan, W., Chen, H., Chen, H., Li, X., 2015a. A theranostic prodrug delivery system based on Pt (IV) conjugated nano-graphene oxide with synergistic effect to enhance the therapeutic efficacy of Pt drug,. Biomaterials 51, 12–21.

Li, N., Yu, L., Wang, J., Gao, X., Chen, Y., Pan, W., Tang, B., 2018. A mitochondria-targeted nanoradiosensitizer activating reactive oxygen species burst for enhanced radiation therapy,. Chem. Sci. 9, 3159–3164.

Li, P., Shi, Y.-w., Li, B.-x., Xu, W.-c., Shi, Z.-l., Zhou, C., Fu, S., 2015b. Photo-thermal effect enhances the efficiency of radiotherapy using Arg-Gly-Asp peptides-conjugated gold nanorods that target αvβ3 in melanoma cancer cells. J. Nanobiotechnol. 13, 1–8.

Li, T., Cao, Y., Li, B., Dai, R., 2021. The biological effects of radiation-induced liver damage and its natural protective medicine,. Prog. Biophys. Mol. Biol. 167, 87–95.

Li, Y., Monteiro-Riviere, N.A., 2016. Mechanisms of cell uptake, inflammatory potential and protein corona effects with gold nanoparticles. Nanomedicine 11, 3185–3203.

Li, Y., Qi, Y., Zhang, H., Xia, Z., Xie, T., Li, W., Zhong, D., Zhu, H., Zhou, M., 2020. Gram-scale synthesis of highly biocompatible and intravenous injectable hafnium oxide nanocrystal with enhanced radiotherapy efficacy for cancer theranostic. Biomaterials 226, 119538.

Liu, F., Lou, J., Hristov, D., 2017. X-Ray responsive nanoparticles with triggered release of nitrite, a precursor of reactive nitrogen species, for enhanced cancer radiosensitization. Nanoscale 9, 14627–14634.

Liu, J., Liang, Y., Liu, T., Li, D., Yang, X., 2015a. Anti-EGFR-conjugated hollow gold nanospheres enhance radiocytotoxic targeting of cervical cancer at megavoltage radiation energies. Nanoscale Res. Lett. 10, 1–12.

Liu, Y., Ji, W., Shergalis, A., Xu, J., Delaney, A.M., Calcaterra, A., Pal, A., Ljungman, M., Neamati, N., Rehemtulla, A., 2019. Activation of the unfolded protein response via inhibition of protein disulfide isomerase decreases the capacity for DNA repair to sensitize glioblastoma to radiotherapy. Cancer Res. 79, 2923–2932.

Liu, Y., Liu, X., Jin, X., He, P., Zheng, X., Dai, Z., Ye, F., Zhao, T., Chen, W., Li, Q., 2015b. The dependence of radiation enhancement effect on the concentration of gold nanoparticles exposed to low-and high-LET radiations,. Phys. Med. 31, 210–218.

Louis, C., Bazzi, R., Marquette, C.A., Bridot, J.-L., Roux, S., Ledoux, G., Mercier, B., Blum, L., Perriat, P., Tillement, O., 2005. Nanosized hybrid particles with double luminescence for biological labeling. Chem. Mater. 17, 1673–1682.

Lovrić, J., Bazzi, H.S., Cuie, Y., Fortin, G.R., Winnik, F.M., Maysinger, D., 2005. Differences in subcellular distribution and toxicity of green and red emitting CdTe quantum dots. J. Mol. Med. 83, 377–385.

Luo, M., Xu, L., Xia, J., Zhao, H., Du, Y., Lei, B., 2020. Synthesis of porous gadolinium oxide nanosheets for cancer therapy and magnetic resonance imaging. Mater. Lett. 265, 127375.

Lux, F., Mignot, A., Mowat, P., Louis, C., Dufort, S., Bernhard, C., Denat, F., Boschetti, F., Brunet, C., Antoine, R., 2011. Ultrasmall rigid particles as multimodal probes for medical applications. Angew. Chem. Int. Ed. 50, 12299–12303.

Lux, F., Tran, V.L., Thomas, E., Dufort, S., Rossetti, F., Martini, M., Truillet, C., Doussineau, T., Bort, G., Denat, F., 2019. AGuIX® from bench to bedside—transfer of an ultrasmall theranostic gadolinium-based nanoparticle to clinical medicine. Br. J. Radiol. 92, 20180365.

Ma, N., Liu, P., He, N., Gu, N., Wu, F.-G., Chen, Z., 2017a. Action of gold nanospikes-based nanoradiosensitizers: cellular internalization, radiotherapy, and autophagy. ACS Appl. Mater. Interfaces 9, 31526–31542.

Ma, N., Wu, F.-G., Zhang, X., Jiang, Y.-W., Jia, H.-R., Wang, H.-Y., Li, Y.-H., Liu, P., Gu, N., Chen, Z., 2017b. Shape-dependent radiosensitization effect of gold nanostructures in cancer radiotherapy: comparison of gold nanoparticles, nanospikes, and nanorods. ACS Appl. Mater. Interfaces 9, 13037–13048.

Ma, X., Gong, N., Zhong, L., Sun, J., Liang, X.-J., 2016. Future of nanotherapeutics: targeting the cellular sub-organelles. Biomaterials 97, 10–21.

Ma, Y.-C., Tang, X.-F., Xu, Y.-C., Jiang, W., Xin, Y.-J., Zhao, W., He, X., Lu, L.-G., Zhan, M.-X., 2021. Nano-enabled coordination platform of bismuth nitrate and cisplatin prodrug potentiates cancer chemoradiotherapy via DNA damage enhancement. Biomater. Sci. 9, 3401–3409.

Macara, I.G., 2001. Transport into and out of the nucleus. Microbiol. Mol. Biol. Rev. 65, 570–594.

Madani, F., Lindberg, S., Langel, Ü., Futaki, S., Gräslund, A., 2011. Mechanisms of cellular uptake of cell-penetrating peptides. J. Biophys. 2011.
Maggiorella, L., Barouch, G., Devaux, C., Pottier, A., Deutsch, E., Bourhis, J., Borghi, E., Levy, L., 2012. Nanoscale radiotherapy with hafnium oxide nanoparticles. Future Oncol. 8, 1167–1181.
Mahmoudi, M., Azadmanesh, K., Shokrgozar, M.A., Journeay, W.S., Laurent, S., 2011a. Effect of nanoparticles on the cell life cycle. Chem. Rev. 111, 3407–3432.
Mahmoudi, M., Lynch, I., Ejtehadi, M.R., Monopoli, M.P., Bombelli, F.B., Laurent, S., 2011b. Protein− nanoparticle interactions: opportunities and challenges. Chem. Rev. 111, 5610–5637.
Mahmoudi, M., Saeedi-Eslami, S.N., Shokrgozar, M.A., Azadmanesh, K., Hassanlou, M., Kalhor, H.R., Burtea, C., Rothen-Rutishauser, B., Laurent, S., Sheibani, S., 2012. Cell "vision": complementary factor of protein corona in nanotoxicology. Nanoscale 4, 5461–5468.
Mao, B.-H., Chen, Z.-Y., Wang, Y.-J., Yan, S.-J., 2018. Silver nanoparticles have lethal and sublethal adverse effects on development and longevity by inducing ROS-mediated stress responses. Sci. Rep. 8, 1–16.
Maravilla, K.R., San-Juan, D., Kim, S.J., Elizondo-Riojas, G., Fink, J.R., Escobar, W., Bag, A., Roberts, D.R., Hao, J., Pitrou, C., Tsiouris, A.J., Herskovits, E., Fiebach, J.B., 2017. Comparison of gadoterate meglumine and gadobutrol in the MRI diagnosis of primary brain tumors: a double-blind randomized controlled intraindividual crossover study (the REMIND study),. Am. J. Neuroradiol. 38, 1681–1688.
Marill, J., Anesary, N.M., Paris, S., 2019. DNA damage enhancement by radiotherapy-activated hafnium oxide nanoparticles improves cGAS-STING pathway activation in human colorectal cancer cells. Radiother. Oncol. 141, 262–266.
Marill, J., Anesary, N.M., Zhang, P., Vivet, S., Borghi, E., Levy, L., Pottier, A., 2014. Hafnium oxide nanoparticles: toward an in vitropredictive biological effect? Radiat. Oncol. 9, 1–11.
Marrache, S., Dhar, S., 2012. Engineering of blended nanoparticle platform for delivery of mitochondria-acting therapeutics. Proc. Natl. Acad. Sci. USA 109, 16288–16293.
McCann, E., O'Sullivan, J., Marcone, S., 2021. Targeting cancer-cell mitochondria and metabolism to improve radiotherapy response. Transl. Oncol. 14, 100905.
McDonald, L., Liu, B., Taraboletti, A., Whiddon, K., Shriver, L.P., Konopka, M., Liu, Q., Pang, Y., 2016. Fluorescent flavonoids for endoplasmic reticulum cell imaging. J. Mater. Chem. B 4, 7902–7908.
McNamara, A., Kam, W., Scales, N., McMahon, S., Bennett, J., Byrne, H., Schuemann, J., Paganetti, H., Banati, R., Kuncic, Z., 2016. Dose enhancement effects to the nucleus and mitochondria from gold nanoparticles in the cytosol. Phys. Med. Biol. 61, 5993.
Miladi, I., Aloy, M.-T., Armandy, E., Mowat, P., Kryza, D., Magné, N., Tillement, O., Lux, F., Billotey, C., Janier, M., 2015. Combining ultrasmall gadolinium-based nanoparticles with photon irradiation overcomes radioresistance of head and neck squamous cell carcinoma, Nanomedicine: Nanotechnology. Biol. Med. 11, 247–257.
Miladi, I., Duc, G.L., Kryza, D., Berniard, A., Mowat, P., Roux, S., Taleb, J., Bonazza, P., Perriat, P., Lux, F., 2013. Biodistribution of ultra small gadolinium-based nanoparticles as theranostic agent: application to brain tumors. J. Biomater. Appl. 28, 385–394.
Milletti, F., 2012. Cell-penetrating peptides: classes, origin, and current landscape. Drug Discov. Today 17, 850–860.
Mowat, P., Mignot, A., Rima, W., Lux, F., Tillement, O., Roulin, C., Dutreix, M., Bechet, D., Huger, S., Humbert, L., 2011. In vitro radiosensitizing effects of ultrasmall gadolinium based particles on tumour cells. J. Nanosci. Nanotechnol. 11, 7833–7839.
Muraca, F., Boselli, L., Castagnola, V., Dawson, K.A., 2020. Ultrasmall gold nanoparticle cellular uptake: influence of transient bionano interactions. ACS Appl. Bio Mater. 3, 3800–3808.
Ng, C.T., Tang, F.M.A., Li, J.J.e., Ong, C., Yung, L.L.Y., Bay, B.H., 2015. Clathrin-mediated endocytosis of gold nanoparticles in vitro. Anat. Rec. 298, 418–427.
Ngoi, N.Y.L., Choong, C., Lee, J., Bellot, G., Wong, A.L.A., Goh, B.C., Pervaiz, S., 2020. Targeting mitochondrial apoptosis to overcome treatment resistance in cancer. Cancers 12, 574.
Ni, K., Lan, G., Chan, C., Quigley, B., Lu, K., Aung, T., Guo, N., La Riviere, P., Weichselbaum, R.R., Lin, W., 2018a. Nanoscale metal-organic frameworks enhance radiotherapy to potentiate checkpoint blockade immunotherapy. Nat. Commun. 9, 1–12.
Ni, K., Lan, G., Veroneau, S.S., Duan, X., Song, Y., Lin, W., 2018b. Nanoscale metal-organic frameworks for mitochondria-targeted radiotherapy-radiodynamic therapy. Nat. Commun. 9, 1–13.
Ninagawa, S., George, G., Mori, K., 2020. Mechanisms of productive folding and endoplasmic reticulum-associated degradation of glycoproteins and non-glycoproteins. Biochim. Biophys. Acta Gen. Subj., 129812
Ohgita, T., Takechi-Haraya, Y., Okada, K., Matsui, S., Takeuchi, M., Saito, C., Nishitsuji, K., Uchimura, K., Kawano, R., Hasegawa, K., 2020. Enhancement of direct membrane penetration of arginine-rich peptides by polyproline II helix structure. Biochim. Biophys. Acta Biomembr. 1862, 183403.
Ojea-Jiménez, I., García-Fernández, L., Lorenzo, J., Puntes, V.F., 2012. Facile preparation of cationic gold nanoparticle-bioconjugates for cell penetration and nuclear targeting. ACS Nano 6, 7692–7702.
Ow, Y.-L.P., Green, D.R., Hao, Z., Mak, T.W., 2008. Cytochrome c: functions beyond respiration. Nat. Rev. Mol. Cell Biol. 9, 532–542.
Ozcelik, S., Pratx, G., 2020. Nuclear-targeted gold nanoparticles enhance cancer cell radiosensitization. Nanotechnology.
Panzarini, E., Mariano, S., Dini, L., 2015. Glycans coated silver nanoparticles induces autophagy and necrosis in HeLa cells. In: Book Glycans Coated Silver Nanoparticles Induces Autophagy and Necrosis in HeLa Cells. AIP Publishing LLC, City, 020017.
Panzarini, E., Mariano, S., Vergallo, C., Carata, E., Fimia, G.M., Mura, F., Rossi, M., Vergaro, V., Ciccarella, G., Corazzari, M., 2017. Glucose capped silver nanoparticles induce cell cycle arrest in HeLa cells, Toxicology. In Vitro 41, 64–74.
Pawlik, T.M., Keyomarsi, K., 2004. Role of cell cycle in mediating sensitivity to radiotherapy. Int. J. Radiat. Oncol. Biol. Phys. 59, 928–942.
Pelkmans, L., Zerial, M., 2005. Kinase-regulated quantal assemblies and kiss-and-run recycling of caveolae. Nature 436, 128–133.
Perera, R.M., Zoncu, R., 2016. The lysosome as a regulatory hub,. Annu. Rev. Cell Dev. Biol. 32, 223–253.
Popken, P., Ghavami, A., Onck, P.R., Poolman, B., Veenhoff, L.M., 2015. Size-dependent leak of soluble and membrane proteins through the yeast nuclear pore complex. Mol. Biol. Cell 26, 1386–1394.
Praefcke, G.J., McMahon, H.T., 2004. The dynamin superfamily: universal membrane tubulation and fission molecules?,. Nat. Rev. Mol. Cell Biol. 5, 133–147.
Qiu, Y., Liu, Y., Wang, L., Xu, L., Bai, R., Ji, Y., Wu, X., Zhao, Y., Li, Y., Chen, C., 2010. Surface chemistry and aspect ratio mediated cellular uptake of Au nanorods. Biomaterials 31, 7606–7619.
Qu, Y., Lu, K., Zheng, Y., Huang, C., Wang, G., Zhang, Y., Yu, Q., 2021. Photothermal scaffolds/surfaces for regulation of cell behaviors. Bioact. Mater.
Ramalho, J., Semelka, R., Ramalho, M., Nunes, R., AlObaidy, M., Castillo, M., 2016. Gadolinium-based contrast agent accumulation and toxicity: an update. Am. J. Neuroradiol. 37, 1192–1198.
Rancoule, C., Magné, N., Vallard, A., Guy, J.-B., Rodriguez-Lafrasse, C., Deutsch, E., Chargari, C., 2016. Nanoparticles in radiation oncology: from bench-side to bedside. Cancer Lett. 375, 256–262.
Reda, M., Ngamcherdtrakul, W., Gu, S., Bejan, D.S., Siriwon, N., Gray, J.W., Yantasee, W., 2019. PLK1 and EGFR targeted nanoparticle as a radiation sensitizer for non-small cell lung cancer. Cancer Lett. 467, 9–18.
Reed, J., Jurgensmeier, J., Matsuyama, S., 1998. Bcl-2 family proteins and mitochondria. Biochim. Biophys. Acta Bioenerg. 1366, 127–137.
Rejman, J., Bragonzi, A., Conese, M., 2005. Role of clathrin-and caveolae-mediated endocytosis in gene transfer mediated by lipo-and polyplexes. Mol. Ther. 12, 468–474.
Rejman, J., Conese, M., Hoekstra, D., 2006. Gene transfer by means of lipo-and polyplexes: role of clathrin and caveolae-mediated endocytosis. J. Liposome Res. 16, 237–247.
Rieck, K., Bromma, K., Sung, W., Bannister, A., Schuemann, J., Chithrani, D.B., 2019. Modulation of gold nanoparticle mediated radiation dose enhancement through synchronization of breast tumor cell population. Br. J. Radiol. 92, 20190283.
Rima, W., Sancey, L., Aloy, M.-T., Armandy, E., Alcantara, G.B., Epicier, T., Malchere, A., Joly-Pottuz, L., Mowat, P., Lux, F., 2013. Internalization pathways into cancer cells of gadolinium-based radiosensitizing nanoparticles. Biomaterials 34, 181–195.
Roa, W., Zhang, X., Guo, L., Shaw, A., Hu, X., Xiong, Y., Gulavita, S., Patel, S., Sun, X., Chen, J., 2009. Gold nanoparticle sensitize radiotherapy of prostate cancer cells by regulation of the cell cycle. Nanotechnology 20, 375101.
Robbins, J., Dilworth, S.M., Laskey, R.A., Dingwall, C., 1991. Two interdependent basic domains in nucleoplasmin nuclear targeting sequence: identification of a class of bipartite nuclear targeting sequence. Cell 64, 615–623.
Ron, D., Walter, P., 2007. Signal integration in the endoplasmic reticulum unfolded protein response. Nat. Rev. Mol. Cell Biol. 8, 519–529.
Rothbard, J.B., Jessop, T.C., Lewis, R.S., Murray, B.A., Wender, P.A., 2004. Role of membrane potential and hydrogen bonding in the mechanism of translocation of guanidinium-rich peptides into cells. J. Am. Chem. Soc. 126, 9506–9507.
Rout, M.P., Aitchison, J.D., Suprapto, A., Hjertaas, K., Zhao, Y., Chait, B.T., 2000. The yeast nuclear pore complexcomposition, architecture, and transport mechanism,. JCB (J. Cell Biol.) 148, 635–652.
Safari, A., Sarikhani, A., Shahbazi-Gahrouei, D., Alamzadeh, Z., Beik, J., Dezfuli, A.S., Mahabadi, V.P., Tohfeh, M., Shakeri-Zadeh, A., 2020. Optimal scheduling of the nanoparticle-mediated cancer photo-thermo-radiotherapy. Photodiagnosis Photodyn. Ther. 32, 102061.
Sancey, L., Kotb, S., Truillet, C., Appaix, F., Marais, A., Thomas, E., van der Sanden, B., Klein, J.-P., Laurent, B., Cottier, M., 2015. Long-term in vivo clearance of gadolinium-based AGuIX nanoparticles and their biocompatibility after systemic injection. ACS Nano 9, 2477–2488.
Savage, K., Lambros, M.B., Robertson, D., Jones, R.L., Jones, C., Mackay, A., James, M., Hornick, J.L., Pereira, E.M., Milanezi, F., 2007. Caveolin 1 is overexpressed and amplified in a subset of basal-like and metaplastic breast carcinomas: a morphologic, ultrastructural, immunohistochemical, and in situ hybridization analysis. Clin. Cancer Res. 13, 90–101.
Schmid, E.M., Ford, M.G., Burtey, A., Praefcke, G.J., Peak-Chew, S.-Y., Mills, I.G., Benmerah, A., McMahon, H.T., 2006. Role of the AP2 β-appendage hub in recruiting partners for clathrin-coated vesicle assembly. PLoS Biol. 4, e262.
Schuemann, J., Bagley, A.F., Berbeco, R., Bromma, K., Butterworth, K.T., Byrne, H.L., Chithrani, B.D., Cho, S.H., Cook, J.R., Favaudon, V., 2020. Roadmap for metal nanoparticles in radiation therapy: current status, translational challenges, and future directions. Phys. Med. Biol. 65, 21RM02.
Setua, S., Ouberai, M., Piccirillo, S.G., Watts, C., Welland, M., 2014. Cisplatin-tethered gold nanospheres for multimodal chemo-radiotherapy of glioblastoma. Nanoscale 6, 10865–10873.
Shao, D., Lu, M.-m., Zhao, Y.-w., Zhang, F., Tan, Y.-f., Zheng, X., Pan, Y., Xiao, X.-a., Wang, Z., Dong, W.-f, 2017. The shape effect of magnetic mesoporous silica nanoparticles on endocytosis, biocompatibility and biodistribution. Acta Biomater. 49, 531–540.
Shen, Z., Liu, T., Yang, Z., Zhou, Z., Tang, W., Fan, W., Liu, Y., Mu, J., Li, L., Bregadze, V. I., 2020. Small-sized gadolinium oxide based nanoparticles for high-efficiency theranostics of orthotopic glioblastoma. Biomaterials, 119783.

Shikata, F., Tokumitsu, H., Ichikawa, H., Fukumori, Y., 2002. In vitro cellular accumulation of gadolinium incorporated into chitosan nanoparticles designed for neutron-capture therapy of cancer. Eur. J. Pharm. Biopharm. 53, 57–63.
Silva, S., Almeida, A.J., Vale, N., 2019. Combination of cell-penetrating peptides with nanoparticles for therapeutic application: a review,. Biomolecules 9, 22.
Smith, S.A., Selby, L.I., Johnston, A.P., Such, G.K., 2018. The endosomal escape of nanoparticles: toward more efficient cellular delivery,. Bioconjugate Chem. 30, 263–272.
Song, Y., Wang, Y., Zhu, Y., Cheng, Y., Wang, Y., Wang, S., Tan, F., Lian, F., Li, N., 2019. Biomodal tumor-targeted and redox-responsive Bi2Se3 hollow nanocubes for MSOT/CT imaging guided synergistic low-temperature photothermal radiotherapy. Advanced healthcare materials 8, 1900250.
Spyratou, E., Makropoulou, M., Mourelatou, E., Demetzos, C., 2012. Biophotonic techniques for manipulation and characterization of drug delivery nanosystems in cancer therapy. Cancer Lett. 327, 111–122.
Štefančíková, L., Lacombe, S., Salado, D., Porcel, E., Pagáčová, E., Tillement, O., Lux, F., Depeš, D., Kozubek, S., Falk, M., 2016. Effect of gadolinium-based nanoparticles on nuclear DNA damage and repair in glioblastoma tumor cells. J. Nanobiotechnol. 14, 63.
Štefančíková, L., Porcel, E., Eustache, P., Li, S., Salado, D., Marco, S., Guerquin-Kern, J.-L., Réfrégiers, M., Tillement, O., Lux, F., 2014. Cell localisation of gadolinium-based nanoparticles and related radiosensitising efficacy in glioblastoma cells. Cancer Nanotechnol. 5, 6.
Suk, J.S., Xu, Q., Kim, N., Hanes, J., Ensign, L.M., 2016. PEGylation as a strategy for improving nanoparticle-based drug and gene delivery. Adv. Drug Deliv. Rev. 99, 28–51.
Sung, H., Ferlay, J., Siegel, R.L., Laversanne, M., Soerjomataram, I., Jemal, A., Bray, F., 2021. Global cancer statistics 2020: GLOBOCAN estimates of incidence and mortality worldwide for 36 cancers in 185 countries. Ca - Cancer J. Clin.
Tang, L., Wei, F., Wu, Y., He, Y., Shi, L., Xiong, F., Gong, Z., Guo, C., Li, X., Deng, H., 2018. Role of metabolism in cancer cell radioresistance and radiosensitization methods. J. Exp. Clin. Cancer Res. 37, 87.
Tang, P.S., Sathiamoorthy, S., Lustig, L.C., Ponzielli, R., Inamoto, I., Penn, L.Z., Shin, J. A., Chan, W.C., 2014. The role of ligand density and size in mediating quantum dot nuclear transport. Small 10, 4182–4192.
Taupin, F., Flaender, M., Delorme, R., Brochard, T., Mayol, J.-F., Arnaud, J., Perriat, P., Sancey, L., Lux, F., Barth, R.F., 2015. Gadolinium nanoparticles and contrast agent as radiation sensitizers. Phys. Med. Biol. 60, 4449.
Taylor, M.J., Perrais, D., Merrifield, C.J., 2011. A high precision survey of the molecular dynamics of mammalian clathrin-mediated endocytosis,. PLoS Biol. 9, e1000604.
Tkachenko, A.G., Xie, H., Coleman, D., Glomm, W., Ryan, J., Anderson, M.F., Franzen, S., Feldheim, D.L., 2003. Multifunctional gold nanoparticle− peptide complexes for nuclear targeting. J. Am. Chem. Soc. 125, 4700–4701.
Tseng, C.-L., Shih, I.-L., Stobinski, L., Lin, F.-H., 2010. Gadolinium hexanedione nanoparticles for stem cell labeling and tracking via magnetic resonance imaging. Biomaterials 31, 5427–5435.
Tsigkou, O., Labbaf, S., Stevens, M.M., Porter, A.E., Jones, J.R., 2014. Monodispersed bioactive glass submicron particles and their effect on bone marrow and adipose tissue-derived stem cells. Advanced healthcare materials 3, 115–125.
Tünnemann, G., Ter-Avetisyan, G., Martin, R.M., Stöckl, M., Herrmann, A., Cardoso, M. C., 2008. Live-cell analysis of cell penetration ability and toxicity of oligo-arginines. J. Peptide Sci.: an official publication of the European Peptide Society 14, 469–476.
Turnbull, T., Douglass, M., Williamson, N.H., Howard, D., Bhardwaj, R., Lawrence, M., Paterson, D.J., Bezak, E., Thierry, B., Kempson, I.M., 2019. Cross-correlative single-cell analysis reveals biological mechanisms of nanoparticle radiosensitization. ACS Nano 13, 5077–5090.
Urra, H., Dufey, E., Avril, T., Chevet, E., Hetz, C., 2016. Endoplasmic reticulum stress and the hallmarks of cancer. Trends in cancer 2, 252–262.
Vakifahmetoglu-Norberg, H., Ouchida, A.T., Norberg, E., 2017. The role of mitochondria in metabolism and cell death,. Biochem. Biophys. Res. Commun. 482, 426–431.
Vergallo, C., Panzarini, E., Carata, E., Ahmadi, M., Mariano, S., Tenuzzo, B.A., Dini, L., 2016. Cytotoxicity of β-D-glucose/sucrose-coated silver nanoparticles depends on cell type, nanoparticles concentration and time of incubation. In: Book Cytotoxicity of β-D-glucose/sucrose-coated Silver Nanoparticles Depends on Cell Type, Nanoparticles Concentration and Time of Incubation. AIP Publishing LLC, City, 020012.
Verry, C., Dufort, S., Barbier, E.L., Montigon, O., Peoc'h, M., Chartier, P., Lux, F., Balosso, J., Tillement, O., Sancey, L., 2016. MRI-guided clinical 6-MV radiosensitization of glioma using a unique gadolinium-based nanoparticles injection. Nanomedicine 11, 2405–2417.
Verry, C., Sancey, L., Dufort, S., Le Duc, G., Mendoza, C., Lux, F., Grand, S., Arnaud, J., Quesada, J.L., Villa, J., 2019. Treatment of multiple brain metastases using gadolinium nanoparticles and radiotherapy: NANO-RAD, a phase I study protocol. BMJ Open 9.
Walczak, A., Gradzik, K., Kabzinski, J., Przybylowska-Sygut, K., Majsterek, I., 2019. The role of the ER-induced UPR pathway and the efficacy of its inhibitors and inducers in the inhibition of tumor progression. Oxid. Med. Cell. Longev. 2019.
Walrant, A., Vogel, A., Correia, I., Lequin, O., Olausson, B.E., Desbat, B., Sagan, S., Alves, I.D., 2012. Membrane interactions of two arginine-rich peptides with different cell internalization capacities. Biochim. Biophys. Acta Biomembr. 1818, 1755–1763.
Wang, C., Li, X., Wang, Y., Liu, Z., Fu, L., Hu, L., 2013a. Enhancement of radiation effect and increase of apoptosis in lung cancer cells by thio-glucose-bound gold nanoparticles at megavoltage radiation energies. J. Nanoparticle Res. 15, 1642.
Wang, F., Yu, L., Monopoli, M.P., Sandin, P., Mahon, E., Salvati, A., Dawson, K.A., 2013b. The biomolecular corona is retained during nanoparticle uptake and protects the cells from the damage induced by cationic nanoparticles until degraded in the lysosomes, Nanomedicine: nanotechnology,. Biol. Med. 9, 1159–1168.
Wang, H., Mu, X., He, H., Zhang, X.-D., 2018. Cancer radiosensitizers. Trends Pharmacol. Sci. 39, 24–48.
Wang, H., Yang, P., Liu, K., Guo, F., Zhang, Y., Zhang, G., Jiang, C., 2008. SARS coronavirus entry into host cells through a novel clathrin-and caveolae-independent endocytic pathway. Cell Res. 18, 290–301.
Wang, L., Zhang, T., Huo, M., Guo, J., Chen, Y., Xu, H., 2019a. Construction of nucleus-targeting iridium nanocrystals for photonic hyperthermia-synergized cancer radiotherapy. Small 15, 1903254.
Wang, Z., Chang, Z.-m., Shao, D., Zhang, F., Chen, F., Li, L., Ge, M.-f., Hu, R., Zheng, X., Wang, Y., 2019b. Janus gold triangle-mesoporous silica nanoplatforms for hypoxia-activated radio-chemo-photothermal therapy of liver cancer. ACS Appl. Mater. Interfaces 11, 34755–34765.
White, B.E., White, M.K., Nima Alsudani, Z.A., Watanabe, F., Biris, A.S., Ali, N., 2022. Cellular uptake of gold nanorods in breast cancer cell lines. Nanomaterials 12, 937.
Williams, R.M., Zhang, X., 2021. Roles of ATM and ATR in DNA double strand breaks and replication stress. Prog. Biophys. Mol. Biol. 161, 27–38.
Wilson III, D.M., Deacon, A.M., Duncton, M.A., Pellicena, P., Georgiadis, M.M., Yeh, A.P., Arvai, A.S., Moiani, D., Tainer, J.A., Das, D., 2021. Fragment-and structure-based drug discovery for developing therapeutic agents targeting the DNA Damage Response. Prog. Biophys. Mol. Biol. 163, 130–142.
Wu, M., Xue, Y., Li, N., Zhao, H., Lei, B., Wang, M., Wang, J., Luo, M., Zhang, C., Du, Y., 2019. Tumor-microenvironment-induced degradation of ultrathin gadolinium oxide nanoscrolls for magnetic-resonance-imaging-monitored, activatable cancer chemotherapy. Angew. Chem. 131, 6954–6959.
Wu, P.-h., Onodera, Y., Ichikawa, Y., Rankin, E.B., Giaccia, A.J., Watanabe, Y., Qian, W., Hashimoto, T., Shirato, H., Nam, J.-M., 2017. Targeting integrins with RGD-conjugated gold nanoparticles in radiotherapy decreases the invasive activity of breast cancer cells. Int. J. Nanomed. 12, 5069.
Xie, A., Li, H., Hao, Y., Zhang, Y., 2021. Tuning the toxicity of reactive oxygen species into advanced tumor therapy. Nanoscale Res. Lett. 16, 1–10.
Xie, X., Liao, J., Shao, X., Li, Q., Lin, Y., 2017. The effect of shape on cellular uptake of gold nanoparticles in the forms of stars, rods, and triangles,. Sci. Rep. 7, 1–9.
Xiong, J., Han, S., Ding, S., He, J., Zhang, H., 2018. Antibody-nanoparticle conjugate constructed with trastuzumab and nanoparticle albumin-bound paclitaxel for targeted therapy of human epidermal growth factor receptor 2-positive gastric cancer. Oncol. Rep. 39, 1396–1404.
Xu, M., Yang, G., Bi, H., Xu, J., Dong, S., Jia, T., Wang, Z., Zhao, R., Sun, Q., Gai, S., 2020. An intelligent nanoplatform for imaging-guided photodynamic/photothermal/chemo-therapy based on upconversion nanoparticles and CuS integrated black phosphorus. Chem. Eng. J. 382, 122822.
Xu, W., Luo, T., Li, P., Zhou, C., Cui, D., Pang, B., Ren, Q., Fu, S., 2012. RGD-conjugated gold nanorods induce radiosensitization in melanoma cancer cells by downregulating αvβ3 expression. Int. J. Nanomed. 7, 915.
Yamazaki, T., Kirchmair, A., Sato, A., Buqué, A., Rybstein, M., Petroni, G., Bloy, N., Finotello, F., Stafford, L., Manzano, E.N., 2020. Mitochondrial DNA drives abscopal responses to radiation that are inhibited by autophagy. Nat. Immunol. 21, 1160–1171.
Yang, C., Uertz, J., Yohan, D., Chithrani, B., 2014. Peptide modified gold nanoparticles for improved cellular uptake, nuclear transport, and intracellular retention. Nanoscale 6, 12026–12033.
Yates, L.A., 2021. Regulation of DNA break repair by RNA. Prog. Biophys. Mol. Biol. 163, 23–33.
Yoo, J., Park, C., Yi, G., Lee, D., Koo, H., 2019. Active targeting strategies using biological ligands for nanoparticle drug delivery systems. Cancers 11, 640.
Zhang, L., Su, H., Wang, H., Li, Q., Li, X., Zhou, C., Xu, J., Chai, Y., Liang, X., Xiong, L., 2019a. Tumor chemo-radiotherapy with rod-shaped and spherical gold nano probes: shape and active targeting both matter. Theranostics 9, 1893.
Zhang, X.-D., Wu, D., Shen, X., Chen, J., Sun, Y.-M., Liu, P.-X., Liang, X.-J., 2012a. Size-dependent radiosensitization of PEG-coated gold nanoparticles for cancer radiation therapy. Biomaterials 33, 6408–6419.
Zhang, X., Wang, H., Coulter, J.A., Yang, R., 2018a. Octaarginine-modified gold nanoparticles enhance the radiosensitivity of human colorectal cancer cell line LS180 to megavoltage radiation. Int. J. Nanomed. 13, 3541.
Zhang, X., Wang, J., Li, X., Wang, D., 2018b. Lysosomes contribute to radioresistance in cancer. Cancer Lett. 439, 39–46.
Zhang, Y., Huang, F., Ren, C., Liu, J., Yang, L., Chen, S., Chang, J., Yang, C., Wang, W., Zhang, C., 2019b. Enhanced radiosensitization by gold nanoparticles with acid-triggered aggregation in cancer radiotherapy. Adv. Sci. 6, 1801806.
Zhang, Y., Xu, D., Li, W., Yu, J., Chen, Y., 2012b. Effect of size, shape, and surface modification on cytotoxicity of gold nanoparticles to human HEp-2 and canine MDCK cells. J. Nanomater. 2012.
Zhao, Z., Xu, K., Fu, C., Liu, H., Lei, M., Bao, J., Fu, A., Yu, Y., Zhang, W., 2019. Interfacial engineered gadolinium oxide nanoparticles for magnetic resonance imaging guided microenvironment-mediated synergetic chemodynamic/photothermal therapy. Biomaterials 219, 119379.
Zhou, S., Zhou, C., Wang, W., Yang, H., Ye, W., 2020. The role of epithelial-mesenchymal transition in regulating radioresistance. Crit. Rev. Oncol.-Hematol., 102961
Zhu, C.-d., Zheng, Q., Wang, L.-x., Xu, H.-F., Tong, J.-l., Zhang, Q.-a., Wan, Y., Wu, J.-q., 2015. Synthesis of novel galactose functionalized gold nanoparticles and its radiosensitizing mechanism. J. Nanobiotechnol. 13, 67.